Evanescent Wave Studies of Interaction and Molecular Recognition at Interface(Dissertation_全文)

AUTHOR(S):

Tanimoto, Satoshi

Evanescent Wave Studies of Interaction and Molecular Recognition at Interface

1997

Satoshi Tanimoto

Table of Contents

Chapter 1

General Introduction

1.1. Introduction

Interface is the boundary between two phases. There exist several kinds of interface such as air-liquid, air-solid, liquid-liquid, liquid-solid, solid-solid. Interface itself has unique structure and character and provides a special field of physico-chemical phenomena. This is due to the fact that the states of atoms and molecules differ from those of bulk phase : the atoms at internal phase undergo isotropic binding forces while those at interface feel anisotropic situation. There are a lot of unique physical and chemical phenomena at interface such as adsorption, electrokinetic phenomena and catalysis etc. Another interesting and important factor is a surface-surface interaction. Especially in the case of colloidal system, the relative surface area of interface is so huge that the interfacial interaction plays an important role in colloid stability, structure formation and other colloidal phenomena.

In a colloidal system, the most important factor to define stability of dispersion is the interaction among the surfaces of colloidal particles. The interactions contain electrostatic and hydrodynamic forces, hydrophobic interaction and so on. Thus the colloidal system has been studied by various methods such as osmotic pressure measurement, viscosity measurement, dynamic light scattering (DLS), X-ray scattering, and electrophoresis. For example, the diffusional behavior of colloidal particles in dispersion has been studied by DLS and the information of influence of ionic atmosphere to diffusion was obtained.[1] By electrophoresis measurement, electrostatic properties of colloidal particles can be estimated.[2] For the colloidal interaction, the structure of colloidal crystal in dispersion has been investigated by small-angle and ultra-small-angle

X-ray scattering methods (SAXS and USAXS).[3,4] The information obtained by these works is extremely important for correct understanding of colloid-colloid and surface-surface interaction, but there is a limit : such scattering experiments just observe a structure as a result of the interaction: the interaction itself could not be measured. In these circumstances, the importance of "direct measurement of interaction" has been attracted keen attentions. By the development of Surface Force Apparatus (SFA) originally proposed by Israelachvili[5] and Atomic Force Microscope (AFM),[6] many trials of "direct measurement of interaction" have been done and interesting results have been coming out. However, one important factor which we should note when we consider colloidal interaction is a motion of colloidal particle. SFA and AFM can detect the force between two surfaces or surface/particle only in steady state: if we like to measure colloidal particle-wall interaction by AFM, we must stick the particle on the cantilever. In this situation, the particle can not move, which is a largely different situation from that in dispersion. On the other hand, there is a reason to believe that the particle motion plays some role for colloid-colloid interaction in dispersion.[7]

In such a situation, a new experimental technique has been required for the study of interfacial phenomena. In 1987, Prieve proposed a new technique using a special kind of surface wave, i.e., evanescent wave.[8] The unique character of evanescent wave will be described in section 1.2 of this chapter. By his idea, interaction between "free" particle and wall in dispersion can be studied.

By application of evanescent wave technique, reactions between colloidal particle and surface can be studied with the combination of fluorescence technique. The kinetics of the reaction can be analyzed by this method. The aim of this thesis is an evaluation of interfacial phenomena by application of evanescent technique.

This thesis consists of two parts. In Part I of this thesis, Evanescent Wave Light Scattering Microscope (EVLSM) was developed and used to study the interaction between particle and surface. EVLSM is an epoch-making apparatus of a combination of evanescent wave and light scattering method, and its details will be described in section 1.3.1. The interaction between colloidal particle and macroscopic surface has been studied as a function of surface charge densities of

the particle, of wall, and as a function of ionic strength of the system. This is a systematic study of particle- surface interaction in colloidal system.

In Part II, the practical investigations were carried out with evanescent wave fluorescence method in addition to the fundamental studies in Part I. Evanescent wave fluorescence method is also known as multiple internal reflection fluorescence (MIRF) and is one of the useful technique to investigate interfacial phenomena.

The most familiar object among colloidal systems is biocolloids, which are components of human bodies. Infinitely large amount of interactions occur in our bodies. In this part, an antigen-antibody reaction was selected among various interactions since this is the one of very important reaction in biology, biochemistry and also in medical science. Although there have been many studies about antigen-antibody interactions, most studies are carried out in bulk phase, i.e., in solution or dispersions and in equilibrium state, but there are few kinetic studies at interface as a field of interaction. It is known that, *in vivo*, the parts recognized as antigen exist on cell surfaces. Hence, it is very meaningful to investigate immunological binding reaction on surface, which is geometrically different from bulk phase but close to real biological system. Part II is concerned with the kinetic study of the relation between binding velocity of antibody and steric structure of antigen at interface with MIRF.

1.2. Basic Principle of Evanescent Wave

At an interface, there are two optical phenomena, reflection and refraction, when light is incident on the boundary between two substances which have different refractive indices (see Fig. 1-1). The refraction can be described by Snell's law eq. (1.1),

$$n_i \sin\theta_i = n_r \sin\theta_r \qquad (1.1)$$

where n_i and n_r are refractive indices of medium 1 and medium 2, θ_i and θ_r the

incidence and refraction angles, respectively.

$$\theta_c = \sin^{-1}(n_r / n_i) \qquad (1.2).$$

While the incident angle is smaller than critical angle θ_c defined by eq. (1.2), the Snell's law holds and the light propagates through the interface as a refracted beam. The incident beam is totally reflected when incident angle becomes larger than the critical angle. In this condition, light is no longer able to propagate beyond the boundary. However, a little component of light exists at the another side of interface even when total reflection occurs. This exuding light is called "evanescent wave".

Evanescent wave, thus generated, has a unique property : the intensity of the wave decays exponentially as a function of the distance from interface where total reflection occurs. In other words, the evanescent wave exists only in the

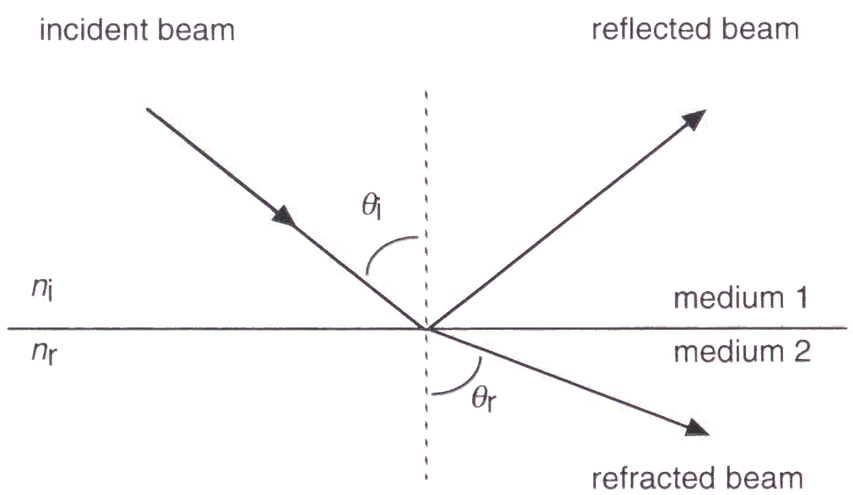

Figure 1-1 Snell's law

vicinity of the interface and creates a region, called "evanescent field". The dimension of the region is of the order of wave length of incident light. (Fig. 1-2)

The existence of evanescent wave has been known since 17th century, and the description about evanescent wave can be found in the book of Sir. Isaac Newton, "Opticks".[9] However, the technological utilization had been scarcely carried out until 1970's, when some applications of evanescent wave to interfacial investigation have started. In these days, various applications are utilized to study interfacial phenomena. Some examples of application, are the attenuated total reflection method (ATR),[10,11] surface plasmon resonance method (SPR),[12,13] and evanescent wave dynamic light scattering (EVDLS).[14] ATR method has been utilized for spectroscopic studies at solid surface with IR or Raman spectroscopy. EVDLS was a relatively-new technique that an evanescent wave was used as an incident light of dynamic light scattering. We have already developed EVDLS technique (Fig. 1-3) and estimated the peculiarity of diffusion behavior of polystyrene latex particles near quartz surface and the region where the

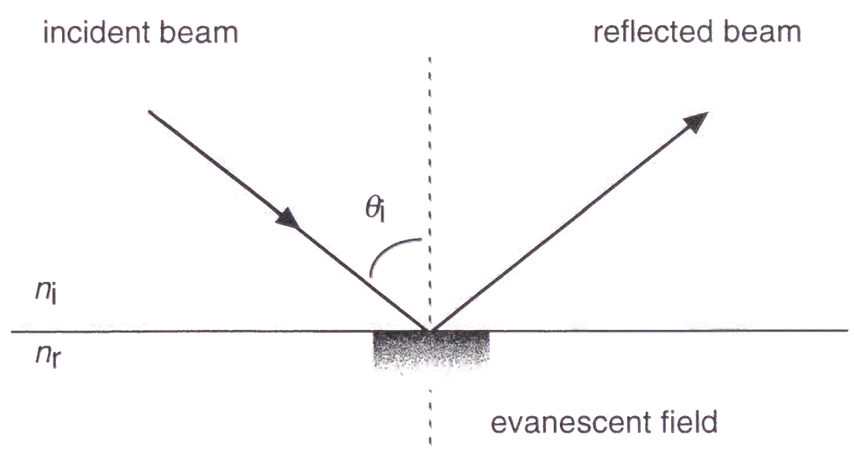

Figure 1-2 Evanescent wave generated by total reflection of light.

electrostatic influences from surface were extended.[14] In section 1.3, the two applications of evanescent wave used in this thesis were described briefly.

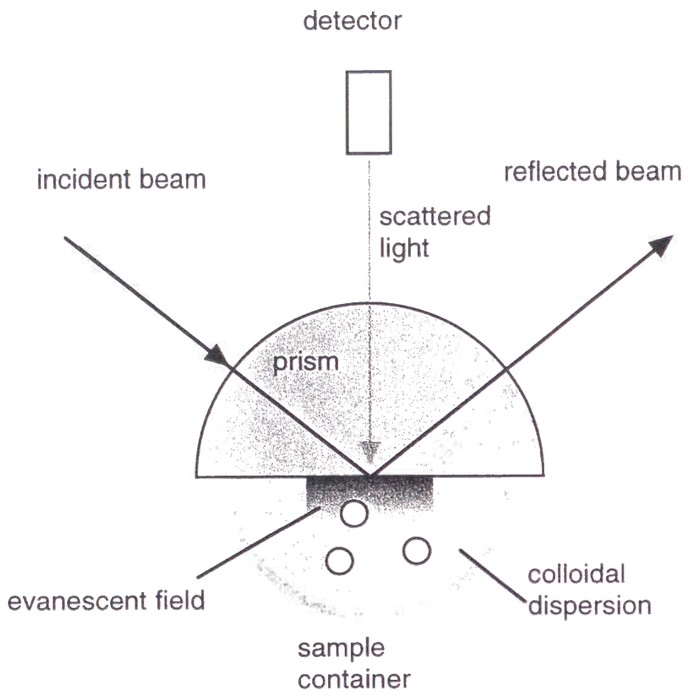

Figure 1-3 Optical arrangements of evanescent wave dynamic light scattering (EVDLS). [ref. 11]

1.3. The Techniques used in this Thesis

1.3.1. Evanescent Wave Light Scattering Microscope Technique (EVLSM).

Evanescent wave light scattering microscope is a new technique by the combination of evanescent wave and light scattering techniques. The apparatus used in this study was constructed in our laboratory by following the principle of Prieve et al.[15] Figure 1-4(a) is the schematic illustration of EVLSM apparatus in our laboratory. This apparatus consists of prism, sample container, microscope, and detector. Evanescent wave is produced in the vicinity of the bottom glass plate of sample container.

The particle, which accidentally comes close to the interface where evanescent field is generated by total reflection, is irradiated strongly by evanescent wave, and the scattered light from the particle is, therefore, intense. As the particle goes away from interface, the intensity of irradiation by evanescent wave decays exponentially and the intensity of scattered light decrease since the scattering intensity is proportional to intensity of incident light. This situation means that the intensity of scattered light is a "measure" of the distance between particle and wall. Hence, the measurement of time-fluctuation of scattered light from only one particle corresponds to the estimation of time-fluctuation of particle-wall distance. The advantage of this technique is that the potential profile of interaction between particle and surface can be directly obtained by estimation of time-fluctuation of distance.

Atomic force microscope (AFM) has been already utilized to measure interaction force between latex particle and mica surface. In this case, one latex particle was fixed with adhesive onto a cantilever as a probe.[16] It is obvious that the condition of particle was different from the free state of actual colloidal dispersion, since the particle in the system was fixed. By contrast, EVLSM can extract the information from the particle of free state. It can be said that EVLSM is one of the ideal methods as a tool for a study of interaction in colloidal system. AFM can obtain interaction "force", however, EVLSM can give us interaction "potential" directly.

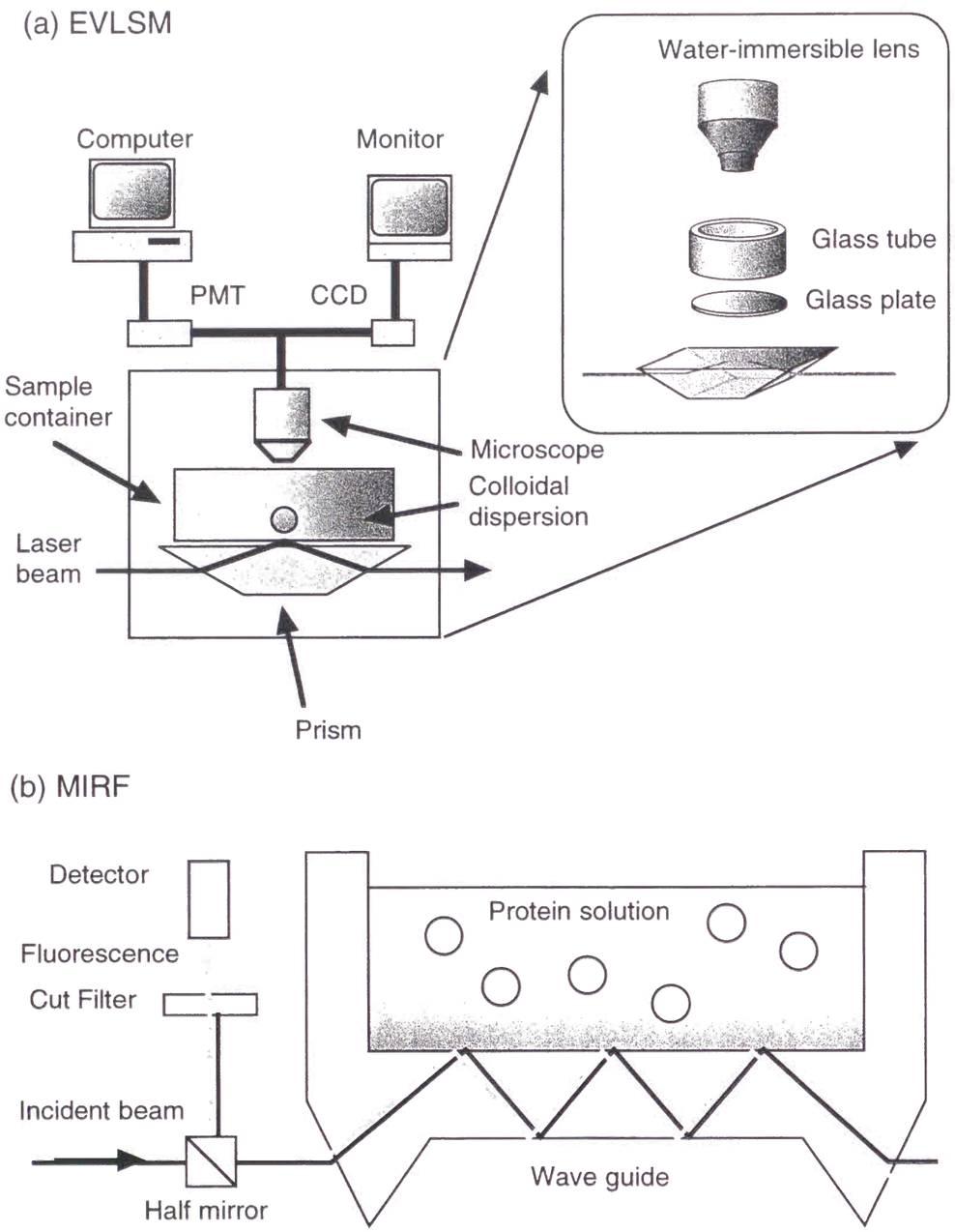

Figure 1-4 Methods used in this thesis, (a) evanescent wave light scattering microscope (EVLSM), (b) evanescent wave fluorescence (MIRF).

1.3.2. Evanescent Wave Fluorescence Method (Multiple Internal Reflection Fluorescence; MIRF).

Evanescent wave fluorescence method (Multiple Internal Reflection Fluorescence method, MIRF) is one of the techniques to investigate adsorption/binding behavior of molecules or particles onto interface.[17] In MIRF, the evanescent wave is used as an excitation beam for fluorescence measurement. The schematic illustration of MIRF is shown in Fig. 1-4(b). The wave guide to generate evanescent wave is made from poly(methyl methacrylate) (PMMA). The incident laser is led into the wave guide and totally reflected by the wall of guide many times; this is the reason why the method is called "multiple internal reflection fluorescence". Evanescent wave generated by this process irradiates only limited space near the interface as described already. Therefore, the chromophore of the sample locating in the evanescent field, i.e., near the interface, is excited and emits fluorescence. From the time-dependence of intensity of fluorescence, kinetic evaluation of various reactions on flat surface becomes possible.

1.4. Outline of this Thesis

This thesis consists of one introductory chapter and two parts. Part I contains Chapters 2, 3, and 4 in which the particle-interface interaction study by EVLSM is described . Part II contains Chapter 5 and 6; the specific interaction of an antigen and its antibody was investigated at a flat plane by MIRF. Brief description of the object studied in each chapter is given below.

In Chapter 2, the particle-interface interaction in a colloidal system, that is, polystyrene latex dispersion, was investigated by EVLSM. The shape of potential profile of interaction was directly estimated by EVLSM and the effect of added salt concentration on the shape of potential profile was duly investigated. At the high added NaCl concentration, the slope of potential well attributed to electrostatic repulsion between particle and glass surface was smaller in comparison with the case at the low salt concentration.

In Chapter 3, the interaction potential was evaluated in the phospholipid

liposome - glass system by EVLSM. The surface charge of phospholipid liposome was controlled by composition change of component lipids. The position of interaction potential well was estimated as a function of surface zeta-potential of liposome particle and as a function of ionic strength of the system. The position of potential minimum shifted toward larger distance from the glass surface with increasing surface zeta-potential of liposome particle and shifted close to surface with increasing ionic strength of the system.

In Chapter 4, EVLSM measurement was carried out for the system of polystyrene latex particle and chemically-modified glass surface. The surface modification was performed with silane-coupling reagent and vinyl monomer having sulfonate group. The surface charge of chemically-modified glass surface was controlled by the reaction time. The position of potential minimum was shifted toward longer distance with increasing zeta-potential of glass surface, indicating enhancement of electrostatic interaction.

In Chapter 5, the specific binding rate of antibody to antigen fixed by physical adsorption on poly(methyl methacrylate) (PMMA) surface was studied by MIRF. Human serum albumin (HSA) and anti-HSA-immunoglobulin G (anti-HSA-IgG) were used as an antigen and its antibody, respectively. The advantage of particle-surface system compared to particle-particle system for observation of immunological reaction is more simple geometry of the system. The relation between immunological binding rate and two dimensional configuration of antigen molecule was discussed. At a low surface concentration of HSA, the initial binding rate of the antibody to the HSA-fixed PMMA surface increased rapidly, and leveled off at a higher surface density. This indicates that the binding of the antibodies is accelerated by increase of the surface antigen density.

In Chapter 6, the antibody binding to antigen-doped lipid monolayer was investigated by MIRF. Dinitrophenyl group (DNP) and anti-DNP-immunoglobulin E (anti-DNP-IgE) were used as a hapten and its antibody, respectively. The hapten-doped lipid monolayer was prepared by Langmuir-Blodgett method on the surface of waveguide and binding kinetics of antibody molecule to this surface was estimated. The system used in this chapter was closer to real biosystem than the system studied in Chapter 5. The relation between binding rate and three dimensional configuration of antigen was

studied. In the case that the position of haptens with spacer was far from the surface of lipid monolayer, the initial binding rate of the antibody to the hapten-doped lipid monolayer was large, which indicates that the binding of the antibodies is affected by the space required for the antibodies to access the haptens.

References

(1) Baur, P.; Nagele, G.; Klein, R. *Phys. Rev. E, Stat. Phys. Plasmas Fluids Relat. Interdiscip. Top.* **1996**, *53*, 6224.

(2) Bastos, D.; de las Nieves, F.*J. Colloid Polym. Sci.* **1993**, *271*, 860.

(3) Matsuoka, H.; Murai, H.; Ise, N. *Phys. Rev. B, Condens. Matter* **1988**, *37*, 1368.

(4) Matsuoka, H.; Nakatani, Y.; Yamakawa, M.; Ise, N. *J. Phys. IV, Colloq.* **1993**, *3*, 451.

(5) For example, Israelachvili, J. N.; Pashley, R. M. *Nature* **1982**, *300*, 341.

(6) Claesson, P.M.; Christenson, H.K. *J. Phys. Chem.* **1988**, *92*, 1650.

(7) Matsuoka, H.; Harada, T.; Kago, K.; Yamaoka, H. *Langmuir* **1996**, *12*, 5588.

(8) Prieve, D. C.; Luo, F.; Lanni, F. *Faraday Discuss. Chem. Soc.* **1987**, *83*, 22.

(9) Newton, I. "Opticks", Dover, New York (1952).

(10) Nakahara, M.; Sanada, Y. *J. Mater. Sci.* **1995**, *30*, 4363.

(11) Harrick, N. J., "Internal Reflection Spectroscopy", John Wiley (1967).

(12) Silin, V.I.; Balchytis, G.A.; Yakovlev, V.A. *Opt. Commun.* **1993**, *97*, 19.

(13) Rahn, J. R.; Hallock, R. B. *Langmuir* **1995**, *11*, 650.

(14) Matsuoka, H.; Morikawa, H.; Tanimoto, S.; Kubota, A.; Naito, Y.; Yamaoka, H. *Colloid Polym. Sci.* to be submitted for publication.

(15) Prieve, D. C.; Frej, N. A. *Langmuir* **1990**, *6*, 396.

(16) Ducker, W.; Senden, T.; Pashley, R. *Langmuir* **1992**, *8*, 1831.

(17) Hasegawa, M.; Kitano, H. *Langmuir* **1992**, *8*, 1582.

Part I

Chapter 2

Direct Estimation of Dynamic Characteristics and Interaction Potential of Latex Particles Interacting with a Glass Surface by Evanescent Wave Light Scattering Microscope Technique

Abstract

The dynamic and static characteristics of a polystyrene latex particle in dispersion interacting with a glass surface were studied by the evanescent wave light scattering microscope (EVLSM) technique originally proposed by Prieve et al. for static studies. The dynamic behavior of the thermal vibration of the particle in a potential well created by electrostatic interaction between the particle and glass and gravity was clearly and quantitatively estimated, in addition to the estimation of the potential profile itself. The potential minimum became shallower with increasing added salt concentration. It was also clearly observed that the vibrational motion of the particle in the well became large in amplitude and that the probability of the occurrence of the large vibration became large with increasing salt concentration. Such information on the dynamics is essential for the correct understanding of the interaction potential. The EVLSM method is shown to be a very powerful technique for the estimation of not only the potential profile but also dynamic characteristics.

2.1. Introduction

An evanescent wave is produced by total reflection of an electromagnetic wave at an interface.[1] When light coming from a medium 2 of refractive index n_2 arrives at the interface with a medium 1 of refractive index n_1 ($n_1 < n_2$), total reflection of the light occurs if the incident angle of the light beam is larger than the critical angle. Under these conditions, an evanescent wave is produced in medium 1 only in the region very close to the interface. This region is typically of the order of the wavelength of the light beam. When a He-Ne laser beam is used as the incident beam, this means that only that part of medium 1 within several thousand Å of the interface is illuminated by the evanescent wave. The depth of this region can be controlled by changing the incident angle of the laser beam, so the evanescent wave can be used as a very powerful tool for extracting information about the interfacial phenomena. Some papers on interfacial studies using a combination of evanescent wave and fluorescence techniques have been published.[2]

An additional unique character of the evanescent wave is the exponential decay of its intensity (strictly speaking, its amplitude) as a function of the distance from the interface, z (see Figure 2-1). By taking advantage of this unique characteristic and by combining it with the light scattering technique, the evanescent wave becomes a powerful tool for studying the behavior of colloidal particles near solid surfaces. For example, Prieve et al.[3-6] have proposed the use of the total internal reflection microscope (TIRM) technique to evaluate the interaction potential between a glass surface and a colloidal particle in a dispersion. We have constructed an evanescent wave light scattering microscope (EVLSM) apparatus following the principle of Prieve et al., and have studied the dynamic and static behavior of a polystyrene latex particle in dispersion interacting with a glass surface. In this paper, we will show that this technique gives us very important information on the dynamic character of the particle, vibrating in a potential well near the interface, in addition to an interaction potential between the particle and the interface.

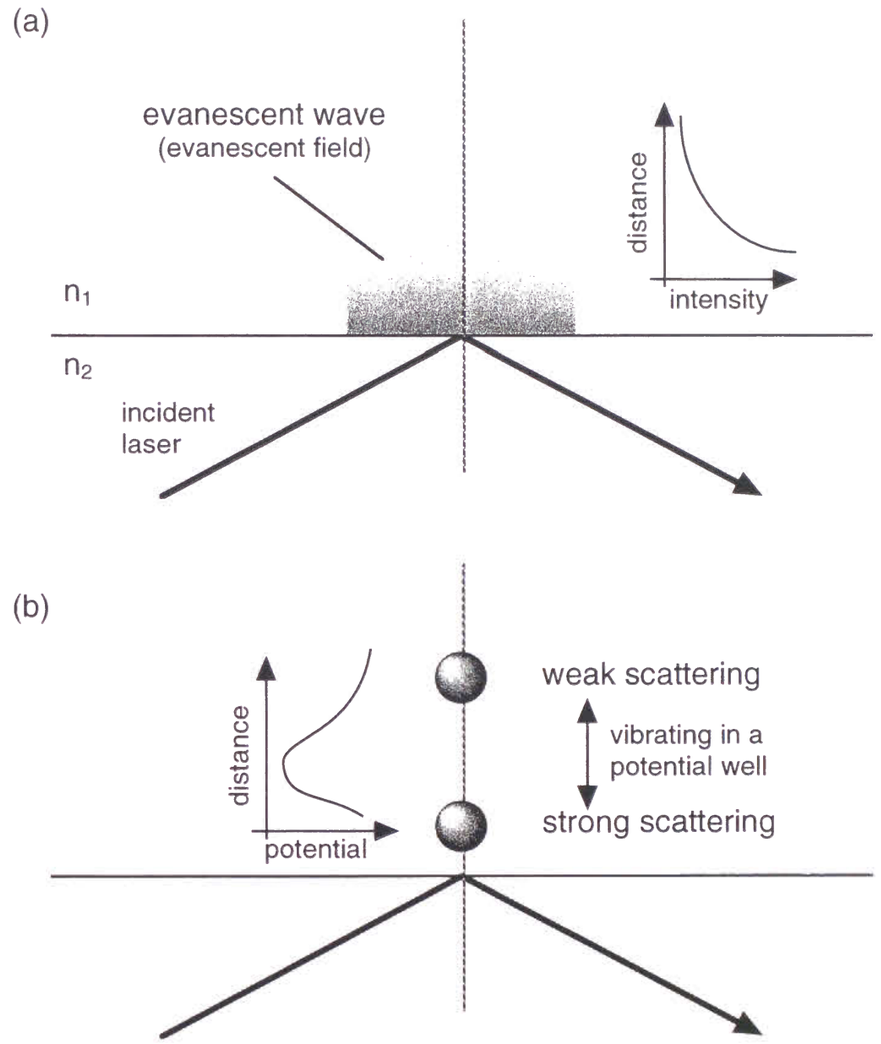

Figure 2-1 (a) Schematic illustration of the characteristics of an evanescent wave and (b) the principle of EVLSM. The intensity of evanescent wave decays exponentially as a function of a distance from interface where total reflection occurs. The particle locating near the interface is scattering evanescent wave strongly.

2.2. Experimental Section

2.2.1. Brief Summary of the Characteristics of Evanescent Waves and the Principle of the Evanescent Wave Light Scattering Microscope Technique.

The characteristics of evanescent waves and the principle of EVLSM are schematically illustrated in Fig. 2-1. An evanescent wave is produced by total reflection of light at the interface of media 1 and 2, whose refractive indices are n_1 and n_2, respectively, with $n_1 < n_2$. The amplitude of the evanescent wave decays exponentially with increasing distance from the interface, z.[1] The intensity of the evanescent wave $I(z)$ is, therefore, expressed as a function of the distance from the total reflection plane, z, as

$$I(z) = I_0 \exp(-2z / \xi) \qquad (2.1)$$

where I_0 is the intensity of the incident beam and the penetration depth ξ is defined by

$$\xi = \lambda_0 / 2\pi n (\sin^2\theta_i - \sin^2\theta_c)^{1/2} \qquad (2.2)$$

where θ_i is the incident angle, θ_c the critical angle, and λ_0 the wavelength of the incident beam in vacuum.

Let us consider the situation in which medium 2 is glass, medium 1 is water, and one latex particle is dispersed in the water. The polystyrene latex particle (specific gravity 1.04) is sedimented down by the effect of gravity if it is sufficiently large. However, since the glass surface is negatively charged (say -30 ~ -40 mV or more in zeta potential[7]), there should be an electrostatic repulsive interaction between the latex particle and the glass surface if the latex particle is negatively charged. These two interactions may form a potential minimum near the interface, and the latex particle may show vibrational motion in this potential well. The distance from the interface z is changing with respect to time due to this vertical vibrational motion. At the same time, the particle is irradiated by evanescent wave. The intensity of the incident evanescent wave depends on z in

the exponential manner which is characterized by ξ. Since the intensity of the scattered light is proportional to that of the incident light, this situation means that the intensity of the scattered light corresponds to the distance z. Hence, if one measures the scattering intensity in a short period many times, the profile of the scattering intensity vs. the number of the observation of the intensity reflects the interaction potential between the particle and the glass surface. This is the principle of EVLSM which was originally proposed by Prieve et al.[3,8] In this chapter, we will show that the raw data obtained by EVLSM clearly displays the vibrational motion of the particle in the potential well, if the intensity of the scattered light can be recorded for the time intervals suitably shorter than the time scale of the thermal vibrational motion.

2.2.2. Sample.

The latex particle used was polystyrene latex (N-1000, Sekisui, Osaka, Japan). Its diameter, provided by the supplier, was 1.026 μm. The sample dispersion (originally 10 vol.%) was purified by dialysis, and then diluted by a factor of about 10^6 in pure water or a salt solution for the EVLSM measurements. The cover glass (Matsunami Glass, 30 x 30 mm) used was treated with sulfonic acid and rinsed with pure water. The water used for the sample preparation was obtained from the Milli-Q system (Bedford, MA). NaCl (analytical grade, Merck, Darmstadt) was used as the added salt. 5mM sodium dodecyl sulfate (Nacalai tesque, Kyoto, Japan) was also present in the sample solution to stabilize the colloidal system.

2.2.3. Apparatus.

The evanescent wave light scattering apparatus was independently constructed in our laboratory by reference to the principle of Prieve et al.[3] A schematic representation of our apparatus is shown in Figure 2-2. A beam from a He-Ne laser (15mW, Nihon Kagaku Engineering, Tokyo, Japan) enters a trapezoidal prism which was specially designed and made (material: BK-7, Sigma Koki, Saitama, Japan). The cover glass of the sample container was set on the upper face of the prism with an index-matched immersion oil, and the laser

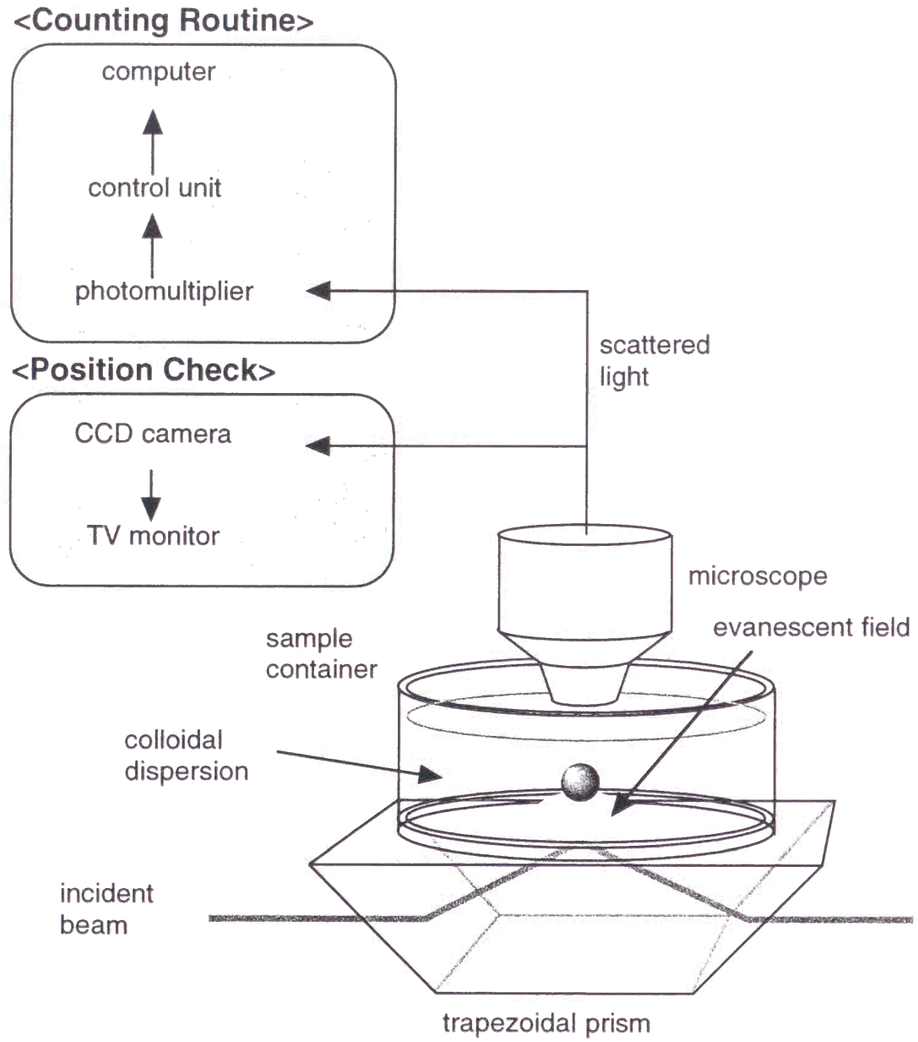

Figure 2-2 Schematic representation of the EVLSM instrument.

beam was totally reflected by the upper interface of the cover glass and the water. In the sample cell, a latex particle is in equilibrium in the potential well caused by the electrostatic interaction with the glass surface and by gravity. It took typically a half or one day to reach equilibrium. After focusing on particles near the bottom of the sample container, a single particle was centered in the field of measurements, which was previously decided, using the translating stage. The scattered light from the particle was collected by a water-immersion lens (×40) attached to the stage-fixed microscope (Optiphot-2 UD, Nikon, Tokyo, Japan). Since the evanescent wave propagates parallel to the interface, the scattering at a scattering angle of 90 degrees was detected by this optical configuration. The scattered light was led to a photomultiplier for the light scattering apparatus (ELS-800, Otsuka Electric, Osaka, Japan) by a multi mode glass fiber (Moritex, Tokyo, Japan). The intensity of the scattered light was collected with a time interval of 2.5 msec. The number of data points for the estimation of the interaction potential was typically 20,000. After finishing one set of measurements, which took about 30 sec., the position of the latex particle in the field of vision was readjusted, and then the next set of the measurements was started.

2.3. Results and Discussion

Figure 2-3 shows the raw data obtained by EVLSM at various salt conditions. The abscissa is the measuring time, and the ordinate is the observed relative intensity for 2.5 msec. Figure 2-4 shows the interaction potential between the latex particle and the glass surface evaluated in the manner of Prieve et al.[3] The potential minimum created by the electrostatic interaction between the particle and the glass wall and gravity is clearly seen. In Fig. 2-3, weak scattering intensity means that z is large, and strong scattering intensity means z is small: the time change of the scattering intensity reflects the vertical motion of the particle. Hence, it can be said that Fig. 2-3 reflects the dynamic character of the particle while Fig. 2-4 reflects the static character. From Fig. 2-3, it is clear that at low ionic strength (Fig. 2-3(a)) the latex particle shows a rather small-amplitude motion in the bottom of the potential well; a larger amplitude motion lasting of

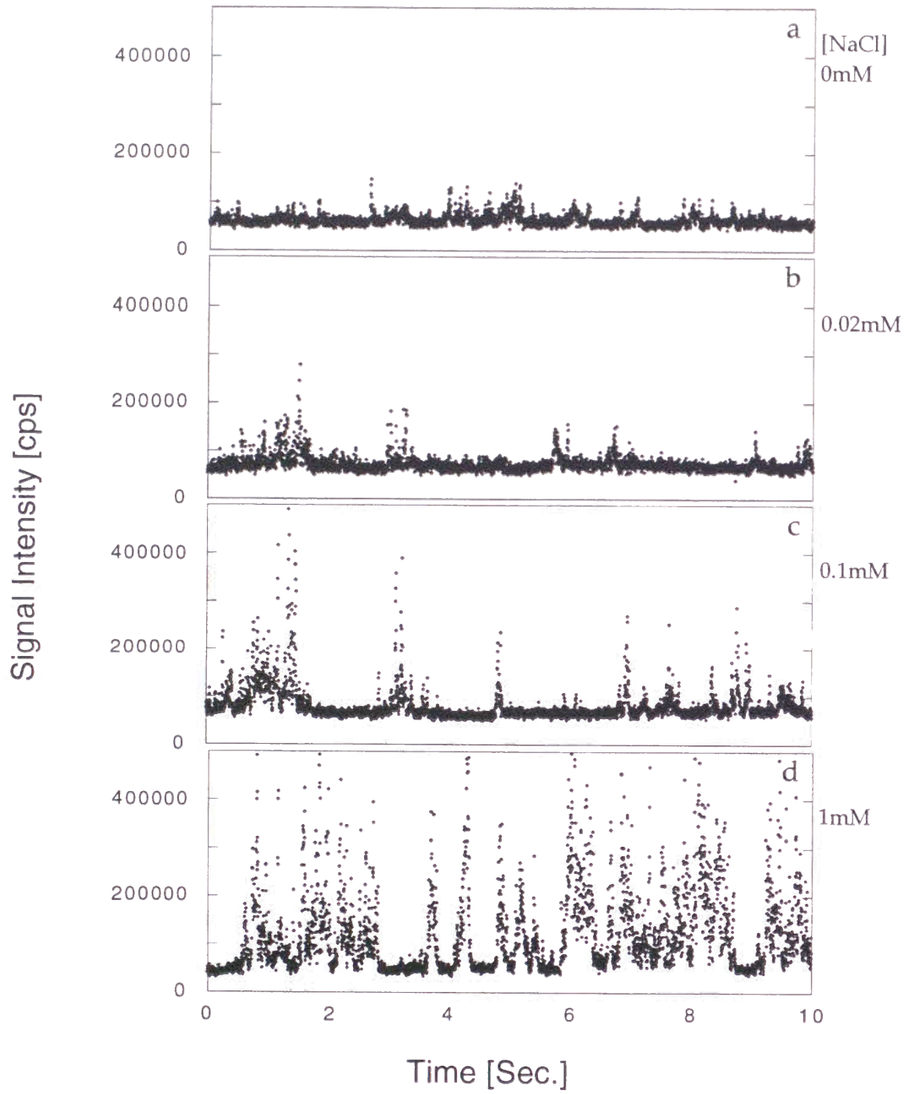

Figure 2-3 The example of raw data obtained from EVLSM
Particle : Polystyrene latex (diameter=1000nm)
Surface : Pyrex glass, Sampling time : 2.5mSec.
Added NaCl conc. : (a)0mM, (b)0.02mM, (c)0.1mM, (d)1mM

the order of 10^{-1} sec. occurred roughly 3 - 5 times in one sec., but it appears to be random. With increasing salt concentration (Fig. 2-3(b) to (d)), the amplitude of the large motion becomes large and the probability of the large motion also increases. This means that the potential well becomes shallower due to the shielding effect of the salt on the electrostatic interaction between the latex particle and the glass surface. This tendency is clearly seen in Fig. 2-4, although the position of the profile is on a relative scale.[10] At the highest salt condition (1 mM, Fig. 2-3(d)), the vibrational motion is very much enhanced; there is a large amplitude and large frequency for the large motion. When there is no added

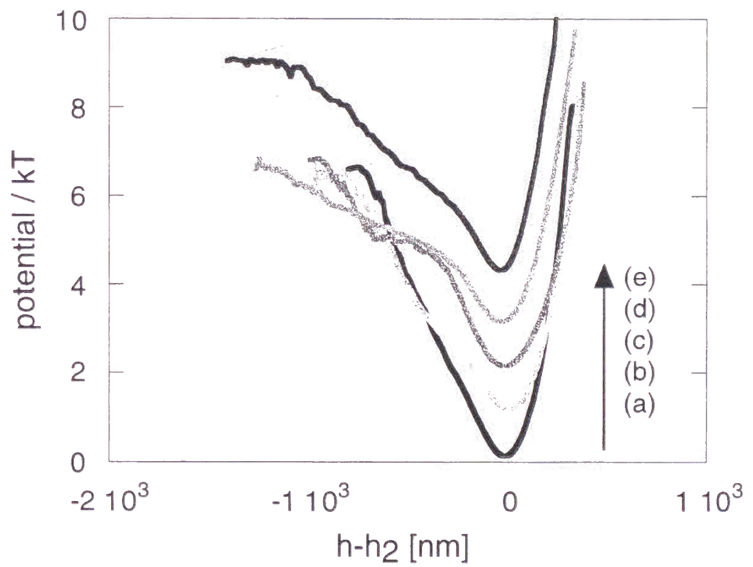

Figure 2-4 The potential profile of interaction between polystyrene latex particle and glass surface at various added NaCl concentrations.
[NaCl] = (a)0, (b)0.01, (c)0.02, (d)0.03, (e)0.1mM
The distance in the ordinate (h-h2) is a relative distance : h normalized to the potential minimum position h2.

NaCl (Fig. 2-3(a)), the particle executes a small vibrational motion near the bottom of the potential well, with a probability of about 80%. By contrast, it executes the large vibrational motion with an approximately 80% probability at 1mM NaCl (Fig. 2-3(d)). For the duration of one large amplitude motion, the difference between the no salt and higher salt conditions is also clearly observable. At 0 mM NaCl, one large vibration consists of about 10 - 20 points, corresponding to 25 - 50 msec. On the other hand, at 1mM NaCl, it consists of about 50 points, indicating that one large vibrational motion lasts for of the order of 100 - 150 msec. By EVLSM, the time scale and dimension of the thermal vibration of the latex particle can be quantitatively determined.

There are some examples of analysis of Brownian motion and the vibrational motion of latex particles in their ordered state in dispersion by a combination of ordinary microscopy with a video device.[12] However, for such a case, the time interval of data collection was typically 1/30 sec, which is insufficient for a detailed analysis of the motion. By EVLSM, this problem can be easily overcome.

2.4. Conclusion

The EVLSM or TIRM technique is a very powerful technique for evaluating the interaction potential between a colloidal particle in dispersion and a solid surface directly. It is very interesting to compare EVLSM results with AFM (Atomic Force Microscope) results. In this study, it has been shown that EVLSM is also an extremely powerful technique for the study of the dynamic behavior of the particle if the sampling time of the measurement is suitably short; this would be difficult to be studied by the AFM technique. It is to be anticipated that much more detailed information about the motion will be obtained by significantly reducing the sampling time. If a measurement is made with time interval of the order of microseconds, a detailed trajectory of the thermal vibrational motion in the potential well may be obtained. In such circumstances, analyses in terms of time-correlation functions and Fourier series would be very interesting. Direct information about the vibrational motion of the particle in the potential well is a very important result for the correct understanding of the interaction potential.

References and Notes

(1) Harrick, N.J., "Internal Reflection Spectroscopy", Interscience, New York, (1967).

(2) Tanimoto, S.; Kitano, H. *Colloids and Surfaces B*, **1995**, *4*, 259.

(3) Prieve, D.C.; Frej, N.A. *Langmuir*, **1990**, *6*, 396.

(4) Bike, S.G.; Prieve, D.C. *Int. J. Multiphase Flow*, **1990**, *16*, 727.

(5) Prieve, D.C.; Bike, S.C.; Frej, N.A. *Faraday Discuss.Chem.Soc.*, **1990**, *90*, 209.

(6) Walz, J.Y.; Prieve, D.C. *Langmuir*, **1992**, *8*, 3073.

(7) Hunter, R.J., "Zeta Potential in Colloid Science", Chap.7, Academic, London, (1988).

(8) Although Prieve et al. call their technique "Total Internal Reflection Microscopy", we suggest the name EVLSM for the following reason. We do not observe "total reflection" by a "microscope", but the scattering from a particle illuminated by an evanescent wave (whose origin is the total reflection) detected by a photomultiplier connected to a microscope. The total reflection is just a tool for producing an evanescent wave. The principle of the technique is scattering of an evanescent wave.

(9) Flicker, S.G.; Bike, S.G. *Langmuir*, **1993**, *9*, 257.

(10) EVLSM measurement on an absolute scale is possible[11] and is now in progress.

(11) Flicker, S.G.; Tipa, J.L.; Bike, S.G. *J.Coll.Int.Sci.*, **1993**, *158*, 317.

(12) Ito, K.; Nakamura, H.; Yoshida, H.; Ise, N. *J.Amer.Chem.Soc.*, **1988**, *110*, 6995.

Chapter 3

Direct Estimation of Interaction Potential between Phospholipid Liposome Particle and Glass Surface by Evanescent Wave Light Scattering Microscope Technique

Abstract

A potential profile of interaction between charged liposome particle and glass surface was estimated directly by Evanescent Wave Light Scattering Microscopy (EVLSM), which can measure the distance between particle and surface as a function of time with interval of the order of less than msec. The minimum of the potential profile, which is a result of electrostatic repulsion and attraction by gravity, was clearly observed. Liposome particles of different surface charge were prepared by using charged and apparently neutral lipid molecules with various mixing ratios. When the amount of minus charges on liposome particle became larger, the position of potential minimum in interaction potential shifted towards larger distance from glass surface, reflecting an increase of electrostatic repulsion between them. The ionic strength dependence of potential profile was also clearly observed. It was confirmed that the electrostatic interaction was an important factor for particle - surface interaction and that EVLSM was a powerful tool for interfacial study in a biocolloidal system.

3.1. Introduction

The one of the important for the correct understanding of fundamental aspects of colloidal phenomena is information of the interaction mechanism between colloidal surfaces. The characteristics of colloidal system has a large contribution of surface phenomena such as surface stability and surface-surface interaction etc., due to the large surface area compared to the molecular systems. These interactions are macroscopic or mesoscopic phenomena. However, it is difficult to extract the peculiarity of surface/interface as a field of interaction in situ because of its microscopic size, since most of conventional experimental techniques can detect almost bulk properties and very little contribution of surface/interface interaction. The minute interaction force is also one of the factor for difficulty. Evanescent wave light scattering microscope (EVLSM) technique is a relatively new method, which has been originally proposed by Prieve et al.[1] EVLSM takes an advantage of evanescent wave, which is a wave located at surface/interface and is produced by total reflection of light.[2] The special characteristics of evanescent wave has been utilized to various surface investigations with combination of other techniques such as fluorescence.[3] EVLSM is a technique by the combination of evanescent wave and light scattering and this can detect the information about the interaction at a surface selectively. The principle of this technique is that any material of unmatched refractive index with medium located near interface, i.e., in evanescent field will scatter light whose intensity is proportional to that of evanescent wave. The data directly obtained by EVLSM can be easily translated into the time dependence of particle - surface distance in the order of ms. or less. Based on the exponential-manner of evanescent wave intensity and an assumption that the distribution of separation distances is described by Boltzmann's distribution, potential energy profiles can be derived. Therefore, the particle-surface interaction potential profile can be directly evaluated by EVLSM. Recently, EVLSM has been utilized for measurements of various systems; Prieve et al., the developer of EVLSM, have proposed the use of the basics of EVLSM, such as colloidal particle-wall interaction, radiation pressure etc.[1,5-7] We have succeeded to construct EVLSM apparatus independently and to evaluate the polystyrene latex particle-glass wall

interaction and the dynamics of latex particle in the potential well, whose details were described in Chapter 2 and publication.[4]

In this work, a systematic study of electrostatic interaction between liposome and glass has been performed by EVLSM. The advantage of liposome system is an easy preparation of particles with different charge. Mixing of apparently neutral (equal number of plus and minus charges) and charged lipid molecules, we can control the charged state of liposome particles. In addition, liposome system is interesting from the point of view of biochemistry since it can be regarded as a model of cell system. We have evaluated the potential profile of liposome-glass system as a function of surface charge in addition to that of ionic strength of the system in detail by EVLSM. Although extensive works have been started for evaluation of particle-wall interaction 'force' by Atomic Force Microscope (AFM),[8] EVLSM gives us another approach to this problem since EVLSM can measure interaction 'potential' directly.

3.2. Theory

3.2.1. Origin of Potential Minimum.

The important factor defining the stability of colloidal dispersion is electrostatic repulsion between charges on colloidal particles. Imagine one system of aqueous colloidal dispersion in glass vessel; when the colloidal particles are negatively charged particles are stabilized by electrostatic repulsion among themselves and glass wall since glass surface is negatively charged in water.[9] At the same time, this particle is drawn by the earth: Gravity. Hence, the particle in dispersion settles down to the bottom glass surface, but becomes in equilibrium since these two forces (electrostatic repulsion between particle and wall and Gravity) form a minimum in the interaction potential. Brownian motion in the vertical direction of this particle is restricted in this potential well. This means that if we know the vertical motion of this particle trapped in the well with appropriate time resolution, we can obtain the potential profile between particle and wall.[1, 4]

3.2.2. Evanescent Wave is ...

When an incident light goes into the boundary between two substances which have different refractive indices and its incident angle is larger than the critical angle, the light is totally reflected at the interface. At this time, an evanescent wave is produced at another side of total reflection plane. The evanescent wave propagates parallel to the interface, and the intensity of this wave from the interface can be expressed as[2]

$$I(z) = I_0 \exp(-2z/\xi) \qquad (3.1)$$

where z is the distance from the interface and I_0 the intensity at the interface, i.e., I_{EV} at $z = 0$, and ξ the "penetration depth", which is a function of the wave length and incident angle, given by

$$\xi = \lambda_0 / 2\pi n (\sin^2\theta_i - \sin^2\theta_c)^{0.5} \qquad (3.2)$$

where λ_0 is the wave length of light in vacuum, θ_i and θ_c are the incident angle and critical angle, respectively, n the refractive index of dispersed medium. Eq. (3.2) means that we can control the penetration depth, ξ, i.e., the range irradiated by evanescent light, by changing the incident angle, θ_i.

Figure 3-1 shows the relation between the relative intensity I_{EV} / I_0 and the distance from interface, at $\xi = 524$ nm. It is clear that the region irradiated by evanescent wave is limited only near the interface, the intensity of evanescent wave at $z = 500$ nm is about 9/50 of that at $z = 0$, and about 1/50 at $z = 1000$ nm. This characteristic property of evanescent wave enables us surface studies.

3.2.3. Principle of Evanescent Wave Light Scattering Technique (EVLSM).

As shown in the previous section, the intensity of evanescent wave has exponential decay rate. This means that particles existing near the interface is irradiated by evanescent wave strongly, and those far away from the interface irradiated less. This situation leads that particles near the interface scatter evanescent light more strongly and those far away scatter more weakly. If we observe only one particle near the interface and this particle moves vertically, we should observe the time-fluctuation of scattering intensity. We can evaluate the time-fluctuation of the distance between surface and particle, as described in the

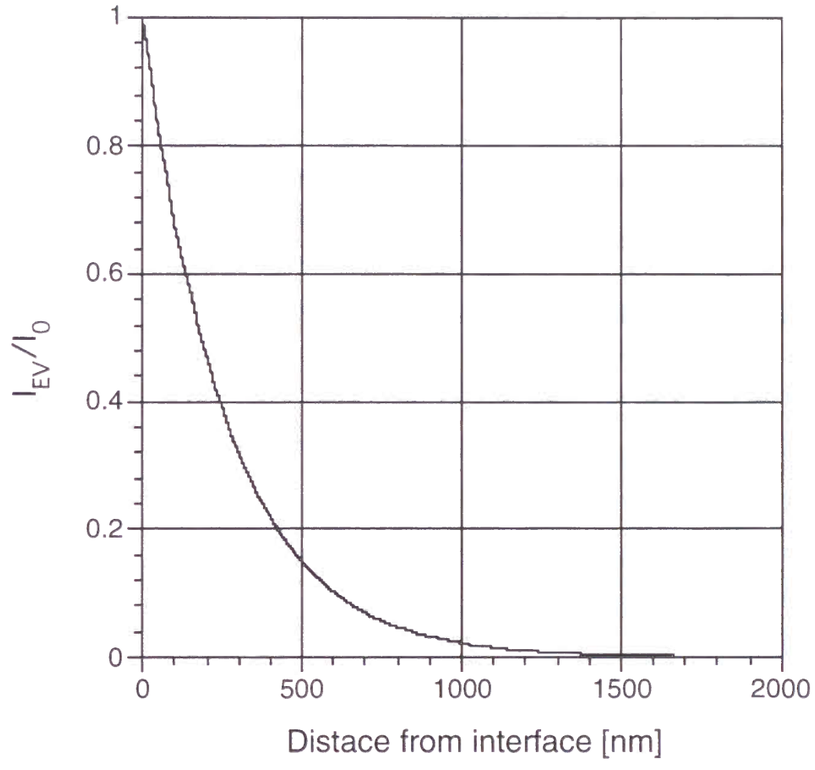

Figure 3-1 Relative intensity of evanescent wave as a function of distance from interface where total reflection occurs. This is an example for the penetration depth of 524 nm.

previous chapter of this thesis.[4]

The particle trapped in the potential well formed near the interface should be vibrating up and down in the well since it has thermal energy. Assuming the distance fluctuation can be described by Boltzmann's distribution, the potential profile is able to be evaluated directly from the scattering intensity fluctuation.[1, 4, 10] The absolute distance between particle and interface can also estimated if one knows I_0 by comparison of the scattering intensity from free particle and that from the particle accidentally-fixed on interface.[11, 12]

Data are collected as scattering intensity, as a function of time, and counted into histogram. The histogram can be then converted into potential energy profile as a function of the distance from interface/surface.[11] Measured scattered light intensity can be translated into separation distance by using eq. (3.3) rewritten from eq. (3.1).

$$z = (\xi/2)\log(I_0/I_{EV}) \qquad (3.3)$$

In the case that the probability of finding a particle at one location is represented by a Boltzmann distribution, the potential energy $V(z)$ relative to that at z_m, $V(z_m)$, is given by

$$(V(z)\text{-}V(z_0))/kT = \ln[N(I(z_0))I(z_0)/N(I(z))I(z)] \qquad (3.4)$$

where z_0 is the distance at which total potential energy is minimum, k Boltzmann's constant, T the absolute temperature of the system, and $N[I(z)]$ the observation number at $I(z)$. The potential is made dimensionless by dividing by kT.

To decide absolute separation distances between the particle and the glass surface, the particle fixed accidentally on the glass surface was observed and the scattering intensity of the particle was used as a standard at z = 650 nm; radius of the liposome particle. The scattering intensity from fixed particle was, therefore, treated as I(650 nm), and this value, z = 650 nm, and ξ (= 524 nm) was substituted to eq. (3.1). As a result, the value I_0 was calculated. After this procedure, the

absolute separation distance between particle and glass surface was obtained using the value, I_0.

3.3. Experimental Section

3.3.1. Preparation of Liposome Suspension.

Lipids used to make liposome suspensions were dipalmitoyl-phosphatidylcholine (DPPC) and dipalmitoylphosphatidylserine (DPPS) (Sigma, St. Louis, MO). The structures of the lipids were shown in Fig. 3-2. The suspensions of liposome were made from the mixture of these lipids by thin layer method (Fig. 3-3).[13] About 25 mg of DPPC and DPPS was weighed out with 4 : 1 or 6 : 1 by mole number and they were solved by 8 ml of chloroform in round-bottomed flask. Chloroform was removed from the solution by rotary evaporator, and the thin layer of lipid mixture on the inner-wall of the flask was obtained. After vaporized completely, 6 ml of water purified by Milli-Q System (Millipore, Bedford, MA) was added in the flask and lipid film swelled in water. Then the flask was shaken violently by Vortex Mixer at 65 ˚C to tear off lipid film from inner wall. By this procedure, suspension of liposome was obtained. The aim of heating is to keep temperature of this system higher than T_c (gel-liquid crystal transition temperature of the lipids) during Vortexing and also to shorten Vortexing time. These procedures are all for preparation of uniformed large liposome particle.

Gel-filtration method was carried out on obtained liposome suspension to fractionate by their size. The gel used was Sephadex G-150 (Pharmacia, Uppsala, Sweden). The size of used column was 2 i.d. x 30 cm, and phosphate buffer (pH 7, 10 mM) was used as a mobile phase. The fractions were collected on the basis of the concentration of filtrate which was detected by UV absorbance. The mean size of liposome particles was investigated by DLS measurement for each fractions, and the fractions of proper size of liposome was altogether and used for EVLSM measurement.

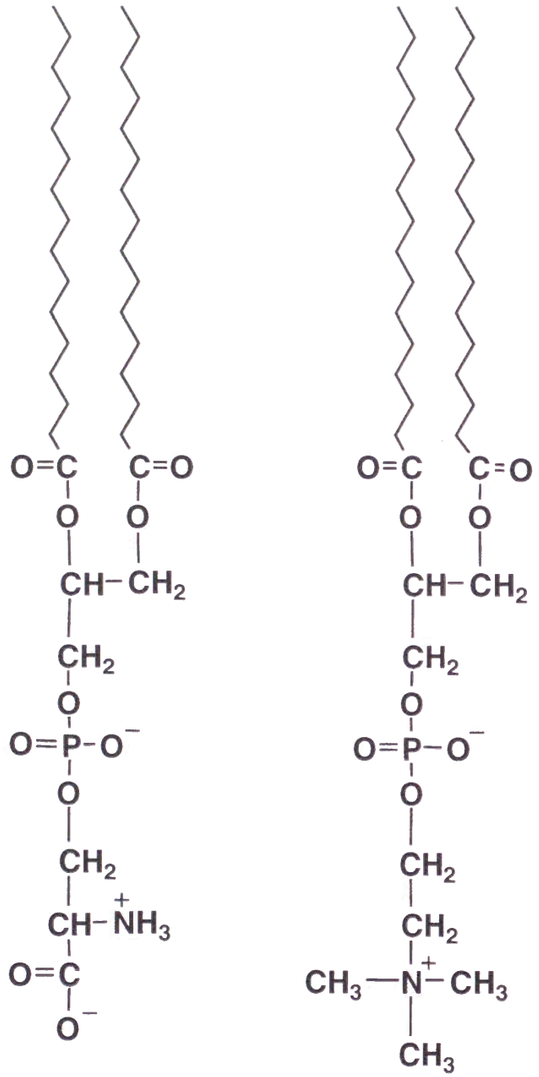

(a) DPPS (b) DPPC

Figure 3-2 Lipids used in this work.
(a) dipalmitoylphosphatidylserine (DPPS)
(b) dipalmitoylphosphatidylcholine (DPPC)

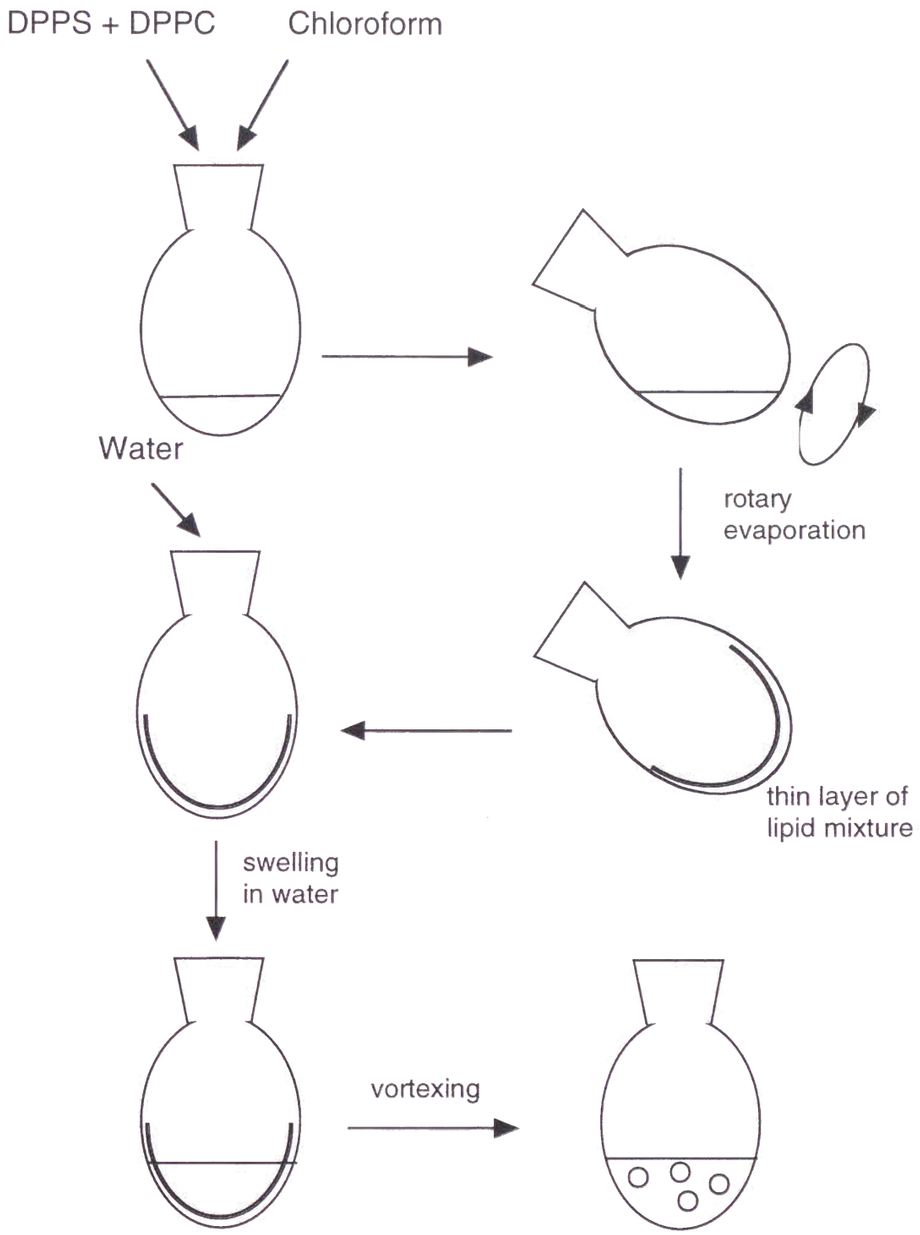

Figure 3-3 The procedure of preparation of liposome suspensions.

3.3.2. Zeta-Potential Measurements.

The zeta-potential of liposome was measured by electrophoretic light scattering method by ELS-800 (Otsuka Electric, Osaka, Japan). The zeta-potential of glass surface was also measured by ELS-800 with the special cell unit for flat surface measurement. Hydroxypropylcellulose-coated polystyrene latex (diameter : 520 nm) was used as a probe particle for surface measurement.

3.3.3. EVLSM Apparatus.

Figure 3-4 shows the outline of EVLSM apparatus. The whole system was constructed in our laboratory on the vibration isolation table (gas-cushioned, Herz, Kanagawa, Japan). The light source was He-Ne laser (15 mW, λ_0 = 632.8 nm, Nihon Kagaku Engineering Co., Ltd., Tokyo, Japan). The trapezoidal prism (upper face: 30 x 25 mm, bottom face: approximately 10 x 25 mm, height: 6 mm, material: BK-7, Sigma-koki, Saitama, Japan) was specially designed for EVLSM apparatus. A glass plate (cover glass usually-used for microscope observation) was glued by Araldite (Ciba-Geigy, Switzerland) onto the bottom of glass tube (diameter: 30 mm, height: 10 mm) and the assortment was used as a sample container. The bottom glass plate was connected on the prism with index-matching oil. The incident beam went into the prism from the side wall, was refracted and totally reflected at the boundary between the upper surface of the bottom glass and sample suspension. By the total reflection, an evanescent wave was generated into the suspension. Liposome suspension was put into the sample container, and kept without disturbance for a day to reach equilibrium. After equilibrium reached, measurement started. After finding one particle swinging in the vicinity of the bottom plate of sample container with microscope (Optiphot-2 UD , Nikon, Tokyo, Japan), the particle was set to the center of field of vision of the microscope by using XY translational stage, which was mounted on the specially designed table. The scattered light from only one particle was caught by microscope and introduced to photomultiplier (PMT, Hamamatsu Photonics, Hamamatsu, Japan). The microscope and the PMT were connected directly by multi-mode glass fiber (material: quartz, diameter of core: 600 μm, Moritex, Tokyo, Japan) with spherical glass lens at each end of the fiber, which was for

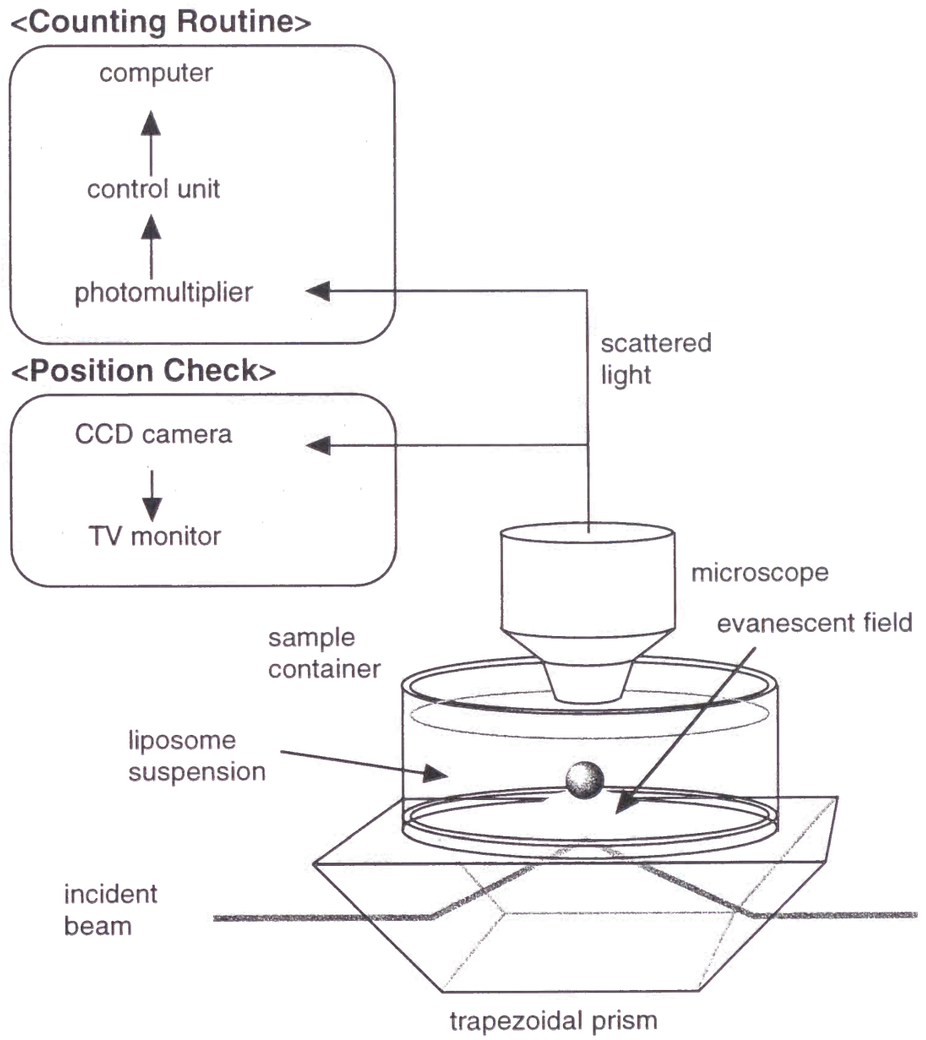

Figure 3-4 Schematic representation of the EVLSM instrument.

reduction of divergence angle of the light. The accumulation time for collection of scattered intensity was 1 msec. and repeated 8192 times continuously (i.e. 8 Sec. for 1 series of measurement). Although the particle moved also X- and Y-direction, no significant displacement from the center of vision of the microscope was detected in this measurement time. There was no dead-time for each 1 msec. measurements, since all the data stored into memory of the control unit (Personal Computer) which was a special technique developed by Otsuka Electric Co. The sampling time selected in our measurement is short enough to discuss fast kinetics of particle motion that can not be obtained with another method such as video observation[14] etc.

3.4. Results and Discussion

3.4.1. Characterization of Liposome.

The preparation of liposome suspension was carried out as described in experimental section. The diameter distribution of obtained liposome was checked by dynamic light scattering (DLS) measurement by ELS-800. On the basis of DLS results, gel-filtration procedure was executed for size fractionation. After these procedure, the mean diameter of liposome was estimated to be 1300 nm by DLS for each liposome suspensions (DPPC : DPPS = 6 : 1 and 4 : 1).

3.4.2. Zeta-Potential of Liposome and Glass Surface.

The zeta-potential of liposome (DPPC : DPPS = 4 : 1) and bottom plate of sample container in phosphate buffer (pH7, ionic strength = 1.20×10^{-4}, 2.75×10^{-4}, 8.25×10^{-4}, 2.42×10^{-3}, 7.90×10^{-3}) was measured by ELS-800. The results were shown in Fig. 3-5 as a function of the ionic strength. The zeta-potential of liposome did not change so much with ionic strength; it was constant at about ζ = -40 mV. However, that of bottom glass changed significantly with ionic strength of buffer in the system. In the case of glass material, it has been known that when the electrolyte in the system increases, zeta-potential of surface becomes less minus value because of the electrostatic shielding effect and adsorption of small ions on the surface.[9] On the other hand, it is guessed that in the case of liposome,

because the surface minus charge of liposome arises from weak acid, that is, carboxyl acid, the buffer effect does work and surface zeta potential did not vary so much.

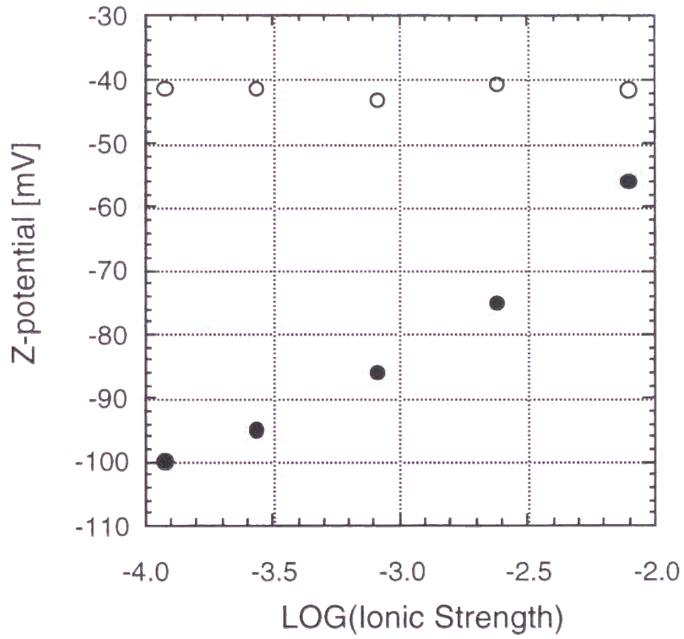

Figure. 3-5 Zeta-potential of glass plate and liposome in various ionic circumstance,.open circle : the surface zeta-potential of liposome particle, closed circle : the surface zeta-potential of glass plate used for sample cell.

3.4.3. EVLSM Measurements.

The raw data set of EVLSM measurement was scattering intensities from one particle counted by PMT during one sampling time, i.e., 1 msec. in this study. The time-fluctuation of scattering intensity of raw data set was directly correlated to the vibrational motion of one liposome particle in the vertical direction.

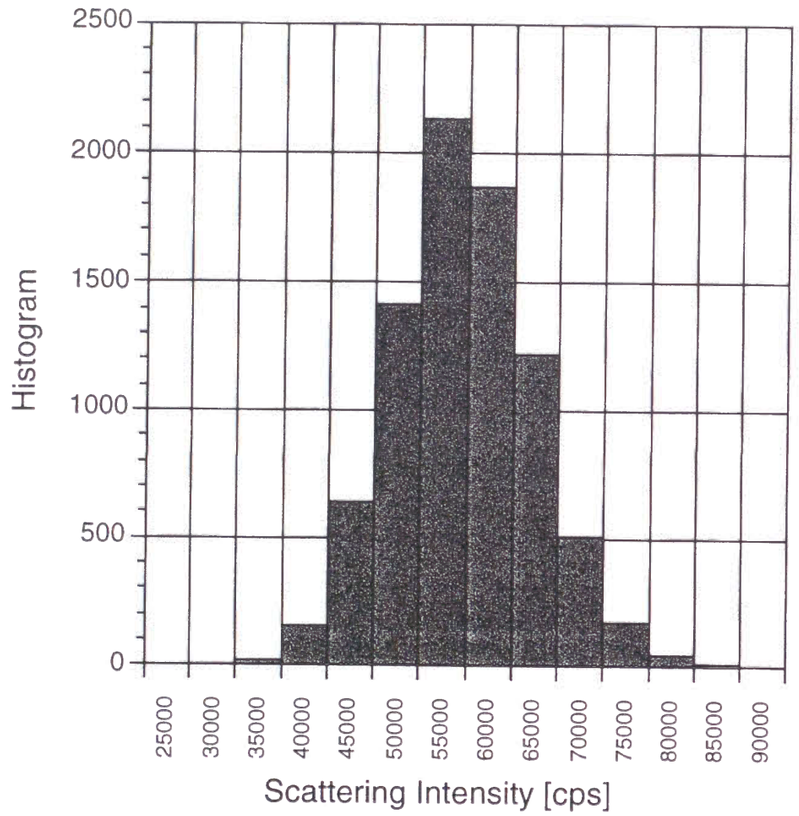

Figure 3-6 An example of scattering intensity histogram obtained by EVLSM. DPPC : DPPS = 4 : 1, diameter = 1300 nm.

From these data, the histogram of frequencies of the number of observation of certain scattering intensity was drawn as a function of scattering intensity.(Fig. 3-6) Since the scattering intensity corresponded to particle-wall distance, the shape of this histogram reflected vertical motion of the particle. The distribution of scattering intensity was able to be converted to the distribution of particle - interface distance as described previously. Therefore, the potential profile of the interaction between liposome and glass surface was derived from the histogram and eq. (3.4).

3.4.4. Potential Profile.

3.4.4.1.The effect of composition of lipids (DPPC and DPPS) in liposome.

We has prepared two kinds of liposome particle by mixing DPPC and DPPS. Since DPPC has one phosphate and one amino groups, this molecule should be apparently neutral. On the other hand, DPPS has carboxyl acid in addition to one phosphate and one amino groups, this should become negative depending on pH value. The liposome particle which contains more DPPS molecules has more negative charges on the surface.

Using EVLSM, the comparison of the potential profiles for these two liposome particles with different-composition (DPPC : DPPS = 4 : 1 and 6 : 1, diameter = 1300 nm for both) was obtained in phosphate buffer (pH7, ionic strength = 1.20×10^{-4}). Typical examples of potential profiles for each liposome were shown as Fig. 3-7(a) and (b). The minimum in the potential profile, which was created by electrostatic repulsion and gravitational force, was clearly observed for each liposome particles. It is clear that the position of potential minimum for liposome which had 20% of DPPS is far apart from interface compared to lower-DPPS-composition liposome (the case of 14% of DPPS). This means that the electrostatic repulsion between liposome and glass surface is enhanced by more minus-charged DPPS on the surface of liposome particle.

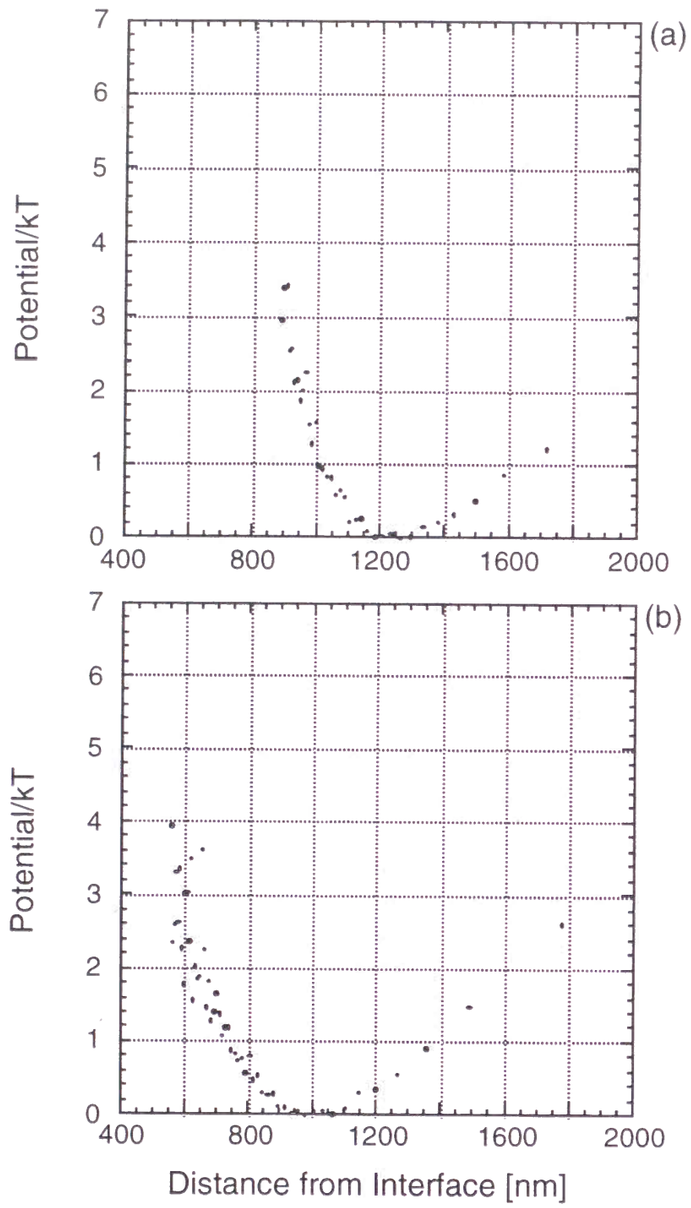

Figure. 3-7 Typical profiles of interaction potential obtained from EVLSM between glass surface and liposome particles of different composition of lipids.
(a) DPPC : DPPS = 4 : 1, diameter = 1300 nm.
(b) DPPC : DPPS = 6 : 1, diameter = 1300 nm.

3.4.4.2.The effect of ionic strength in the system.

The potential profiles of liposome (d = 1300 nm, DPPC : DPPS = 4 : 1) were obtained at five different ionic strengths of buffer (pH7, ionic strength = 1.20×10^{-4}, 2.75×10^{-4}, 8.25×10^{-4}, 2.42×10^{-3}, 7.90×10^{-3}). In Fig. 3-8 the distribution of

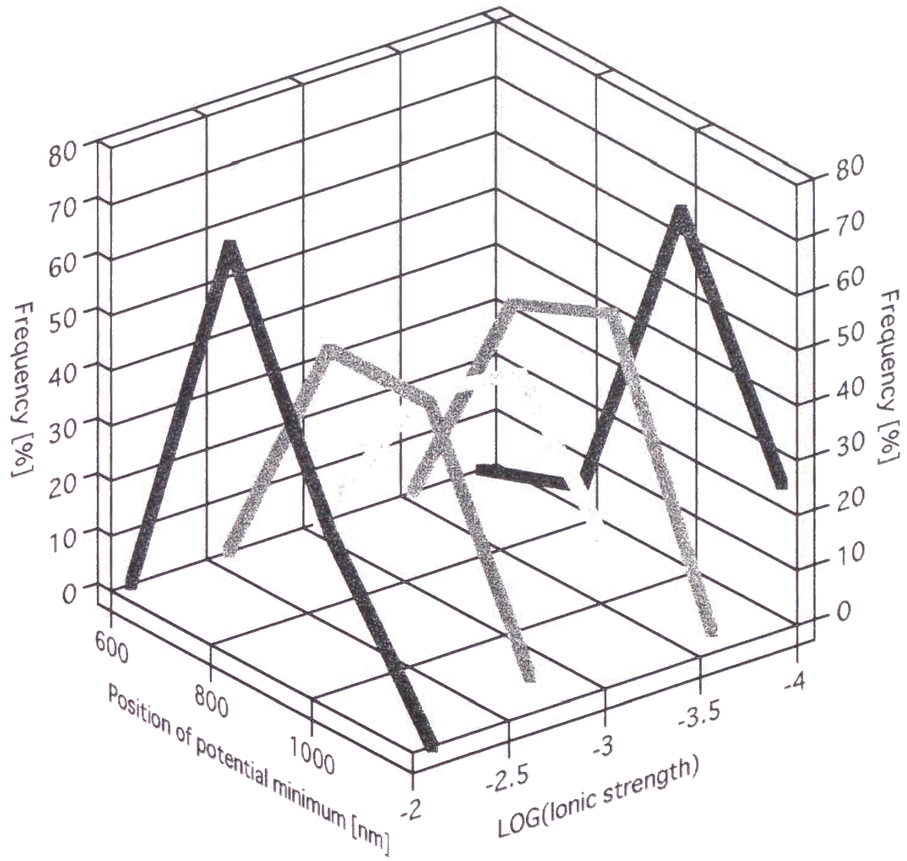

Figure 3-8 Distributions of position of potential minimum as a function of ionic strength in the system. DPPC : DPPS = 4 : 1, diameter = 1300 nm.

minimum positions were shown as a function of ionic strength of buffer. Since the minimum position fluctuated a little bit for each measurement, we repeated the same measurement many times (typically 15 times), and the frequency (number of observation) of minimum position was plotted for every 200 nm. It was seen that the peak of minimum position distribution shifted toward near the glass surface with increasing ionic strength in the system. At the ionic strength of 7.9×10^{-3}, the most probable position was about 800 nm from the glass surface. On the other hand, at the ionic strength of 1.2×10^{-4} the peak of plots shifted to about 1000 nm. We should take at least two factors into account for interpretation of this peak shift. The first is the shielding effect of liposome - glass electrostatic repulsion, which should be enhanced with increasing ionic strength in the system. The other is the change of zeta-potential of glass surface with the change of ionic strength. As shown in Fig. 3-5, the ζ-potential of glass surface reduced with increasing ionic strength. This reduction should lead weak electrostatic repulsion with liposome particle, which results in the closer minimum position of the glass-liposome interaction potential since gravitational force is not affected by electrostatic condition of the system. This is what we observed quantitatively by EVLSM technique, directly.

3.5. Conclusion

It has shown that EVLSM is a powerful tool to estimate electrostatic forces between a colloidal particle and a flat surface. The potential profiles of interaction between phospholipid liposome of diameter 1300 nm and glass flat plate in phosphate buffer were estimated as a function of surface charge and ionic strength.

These profiles demonstrated the influence of electrostatic repulsion on the vertical motion of the spheres interacting with glass wall in suspension. The position of potential minimum became closer to the surface with decreasing particle charge and increasing ionic strength.

In addition, the absolute value for the distance between particle and wall could be estimated in this study. The charge of the minimum position could be

discussed in absolute scale. Although some unclear points for EVLSM technique have been pointed out, such as the relatively larger particle size compared to the wave length and the penetration depth, all the data that we have obtained are reasonable from the point of view of electrostatic interaction. The next step may be more quantitative discussion with colloidal interaction theories, which is now in progress.

Another possibility for application of EVLSM may be an estimation of external forces. In this study, the external force was gravity. This can be another force such as electric field, magnetic field etc., and these forces can be evaluated by EVLSM, if necessary. A part of such experiments is already done in our laboratory. In the present liposome-glass system, the electrostatic interaction was detected by EVLSM since it is the dominant factor. Other interaction should be detected, if it is dominant, such as hydrogen-bonding, antigen-antibody interaction, especially in biological systems.

Recently, AFM is extensively applied to measure particle-surface forces in addition to surface imaging.[8] They glued one colloidal particle to the cantilever and measured the force. In EVLSM, the interaction potential can be estimated without fixing particle, that is, we can measure interaction for the particle in free state. This is a great advantage of EVLSM compared to the AFM since it has been clarified gradually that the dynamic properties of colloidal particle and/or counterions play an important role in the electro'static' interaction.[15]

References

(1) Prieve, D.C.; Frej, N.A. *Langmuir*, **1990**, *6*, 396.
(2) Harrick, N.J., Internal Reflection Spectroscopy, Interscience, New York, (1967).
(3) Tanimoto, S.; Kitano, H. *Colloids and Surfaces B*, **1995**, *4*, 259.
(4) Tanimoto, S.; Matsuoka H.; Yamaoka, H. *Colloid Polym. Sci.*, **1995**, *273*, 1201.
(5) Bike, S.G.; Prieve, D.C. *Int. J. Multiphase Flow*, **1990**, *16*, 727.
(6) Prieve, D.C.; Bike, S.C.; Frej, N.A. *Faraday Discuss.Chem.Soc.*, **1990**, *90*, 209.
(7) Walz, J.Y.; Prieve, D.C. *Langmuir*, **1992**, *8*, 3073.
(8) For example, Braithwaite, G.J.C.; Howe, A.; Luckham, P.F. *Langmuir*, **1996**, *12*, 4224.
(9) Hunter, R.J., "Zeta Potential in Colloid Science", Chap.7, Academic, London, (1988).
(10) Flicker, S.G.; Bike, S.G. *Langmuir*, **1993**, *9*, 257.
(11) Flicker, S.G.; Tipa, J.L.; Bike, S.G. *J.Coll.Int.Sci.*, **1993**, *158*, 317.
(12) Tanimoto, S.; Yamauchi, H.; Matsuoka, H.; Yamaoka, H. *Polymer Preprints*, **1997**, *46*, 894.
(13) Bangham, A.D.; Standish, M.M.; Watkins, J.C. *J. Mol. Biol.*, **1965**, *13*, 238.
(14) Ito, K.; Nakamura, H.; Yoshida, H.; Ise, N. *J.Amer.Chem.Soc.*, **1988**, *110*, 6995.
(15) Matsuoka, H.; Harada, T.; Kago, K.; Yamaoka, H. *Langmuir*, **1996**, *12*, 5588.

Chapter 4

Estimation of Interaction between Colloidal Particle and Chemically-modified Glass Surface by Evanescent Wave Light Scattering Microscope Technique (EVLSM)

Abstract

The profile of interaction potential between polystyrene latex particle and chemically-modified glass surface was estimated directly by Evanescent Wave Light Scattering Microscope (EVLSM) Method, which can measure the distance between particle and surface as a function of time with interval of the order of less than ms. The minimum of the potential profile, which is a result of an electrostatic repulsion and an apparent attraction by gravity, was clearly observed. Glass surface was chemically modified by treatment with silanization reagent and vinyl monomer having sulfonate group. When the absolute value of zeta potential of the glass surface became larger, the position of potential minimum on interaction potential shifted toward larger distance from glass surface, reflecting an increase of electrostatic repulsion between particle and wall. The ionic strength dependence of potential profile was also clearly observed. It was confirmed that EVLSM was a powerful tool for quantitative estimation of particle-wall interaction.

4.1. Introduction

Interface is the special field where various reactions and interactions occur. Its characteristic properties such as surface structure, roughness, surface charge density, and hydrophobicity etc. are important factors which can define the property of dispersion. In the case of colloidal dispersion in water, the stability is governed by the properties of colloidal particle surface, such as the electrostatic character and hydrophobicity and by the ionic strength of disperse medium. Hence, it is very important to extract information only near surface or interface. Extensive attempts to throw light on interfacial phenomena have been done. However, because of experimental difficulties, there were few reports on extraction of interfacial information from the raw experimental data.

In our laboratory, interfacial phenomena and surface structure have been studied in detail by using various methods such as X-ray reflectivity (XR),[1,2,3,4] atomic force microscope (AFM), and evanescent wave light scattering microscope technique (EVLSM).[5] XR measurement is used for structural analysis of surface and interface in multilayer system, such as polymer film prepared by spin-coating and Langmuir-Blodgett (LB) lipid monolayer deposited on solid substrate or water surface. The wave length of X-ray used in our laboratory is 1.54 Å, so the structure of surface and interface can be evaluated in the order of angstrom. Atomic force microscope (AFM) is now the most popular technique among various scanning probe microscopies (SPM). SPM is a powerful tool to obtain the information for surface structure like the molecular arrangement or orientation in an atomic order. Many workers have reported scanning tunnel microscope (STM) and AFM images for LB multilayer and monolayer and adsorbed monolayers of amphiphilic substances such as phospholipids and block copolymers.

AFM can give us 2D surface images by direct measurement of intersurface force between scanning tip and investigated objects. Recently using AFM, extensive works for direct evaluation of particle-wall interaction force[6] have been started by attaching a particle on cantilever. On the other hand, recently the evanescent wave is used to study various surface phenomena since it has special property that it exists only near the surface.[7,8] EVLSM is a relatively new technique of a combination of evanescent wave and light scattering techniques. It has been used to estimate interaction potential between colloidal particle and glass wall in dispersion system.[5,9,13] We have succeeded to construct EVLSM apparatus independently[5] by following the principle of Prieve et al.[9] In EVLSM, the particle is observed near the bottom plane of sample container. In the case of negatively charged colloidal particle-glass wall system in water, the particle is pushed upward by electrostatic repulsion, which was an important factor of stability in colloidal systems. At the same time, the particle is pulled downward by the gravity. Hence, the potential profile obtained by EVLSM showed one minimum formed by these two forces. We have already reported interaction potential profile between particle and surface in some systems; polystyrene latex particle and phospholipid liposome particle - naked glass surfaces.[5,10] Recently, EVLSM has been used for various measurements such as particle-wall interaction, radiation pressure etc.[11,12,13]

The character of interaction between colloidal particle and macroscopic surface was defined as a function of surface charge densities of the particle, of wall, and ionic strength of the system. We have already studied the effect of particle charge density and of ionic strength of the disperse medium on the particle - surface interaction.[5,10] In this chapter, the author has investigated interaction potential between polystyrene latex particle and chemically modified glass surface by using EVLSM to check the effect of charge density of surface on interaction. The chemical surface modification was introduced to change the electrostatic nature of the glass surface: sulfonate groups were fixed chemically on the surface. The relation between the position of potential minimum and the surface zeta-potential of chemically-modified glass surface is investigated in detail. Since the effect of gravity is invariant, the change of potential minimum evaluated by EVLSM reflects the effect of electrostatic nature only.

4.2. Experimental Section

4.2.1. Brief Review of the Character of Evanescent Wave.

Evanescent wave is the special wave generated by total reflection of light at the interface.[14] The description of its existence could be found in the book of Sir. Isaac Newton "Opticks".[15] However, the experimental utilization of evanescent wave has been never done for a long time.

When an incident light goes into the boundary between two substances which have different refractive indices and its incident angle is larger than the critical angle, the light is totally reflected at the interface. At this time, the evanescent wave is produced at opposite side of total reflection plane. The evanescent wave propagates parallel to the interface, and the intensity of this wave at a distance z from the interface can be expressed exponentially as[14]

$$I(z) = I_0 \exp(-2z / \xi) \qquad (4.1)$$

where z is the distance from the interface, I_0 the intensity at the interface i.e., I_{EV} at $z = 0$, and ξ the "penetration depth of evanescent wave", which is a function of the wave length and incident angle, given by

$$\xi = \lambda_0 / 2\pi n (\sin^2\theta_i - \sin^2\theta_c)^{0.5} \qquad (4.2)$$

where λ_0 is the wave length of light in vacuum, θ_i and θ_c are the incident angle and critical angle of the interface, respectively, n the refractive index of disperse medium. Eq. (4.2) indicates that we can control the penetration depth, ξ, i.e., the range irradiated by evanescent light, by changing the incident angle, θ_i.

Figure 4-1 shows the relation between the relative intensity I_{EV}/I_0 and the distance from the interface, at ξ = 524 nm. The figure makes it clear that the region irradiated by evanescent wave is limited only near the interface, the intensity of evanescent wave at z = 500 nm is about 9/50 of that at $z = 0$, and about 1/50 at z = 1000 nm. This characteristic property of evanescent wave enables us to

study peculiarities of surfaces.

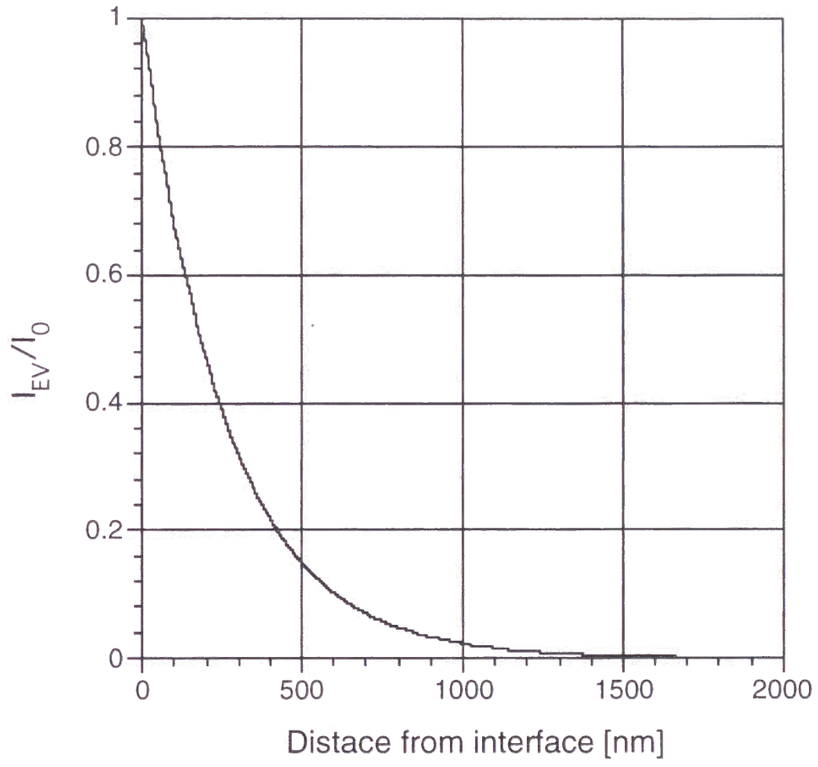

Figure 4-1 Relative intensity of evanescent wave as a function of distance from interface where total reflection occurs. This is an example for the penetration depth of 524 nm.

4.2.2. Principle and Apparatus of EVLSM.

The stability of colloidal dispersions is governed by electrostatic repulsion between charges on the surface of colloidal particles. Imagine one system of aqueous colloidal dispersion in glass vessel; when colloidal particles are negatively charged, the negatively charged particles existing near the bottom plane of the vessel are pushed upward by electrostatic repulsion of glass wall since glass surface is also charged negatively in water.[16] At the same time, the particles are drawn downward by the earth : Gravity. Hence, by these two forces a potential well is formed in the vicinity of the glass surface and the particle which settles down to the bottom of the vessel will be captured in the well. EVLSM can be applied to such condition.

Schematic illustration of EVLSM apparatus is shown as Fig. 4-2. All components were set on the vibration-isolated table. A He-Ne laser (λ = 632.8 nm) was used in this work. The trapezoidal prism was designed and made from optical glass, BK-7, for the special purpose to generate evanescent wave. The sample container was assembled from glass tube and bottom glass plate with adhesive, and was attached onto the prism with index matching oil.

The incident beam went into the side wall of the prism. After refraction, it went in the prism and then hit the boundary between colloidal dispersion and bottom glass plate of sample container. The beam was reflected at the interface, and the evanescent wave was produced beyond the boundary where total reflection occurred. Latex particles which were existing near the interface, i.e., in the evanescent field, were irradiated by the evanescent wave and scatter it. Only one particle was caught by microscope and its scattering intensity was measured repeatedly with short time interval. The time-fluctuation of scattering intensity must reflect the time-fluctuation of distance between particle and plane. Microscope image was used to check the horizontal position of particle and to collect the scattered light from only one particle. The scattered light was lead to photomultiplier (Hamamatsu Photonics, Hamamatsu, Japan) through the optical fiber and was counted. In this thesis, the sampling period is 1 msec. and the data gathering is carried out 4000 or 8000 times for one series of measurement. The sampling time used in this measurement is short enough to discuss fast kinetics of particle motion that can not be obtained with another method such as video

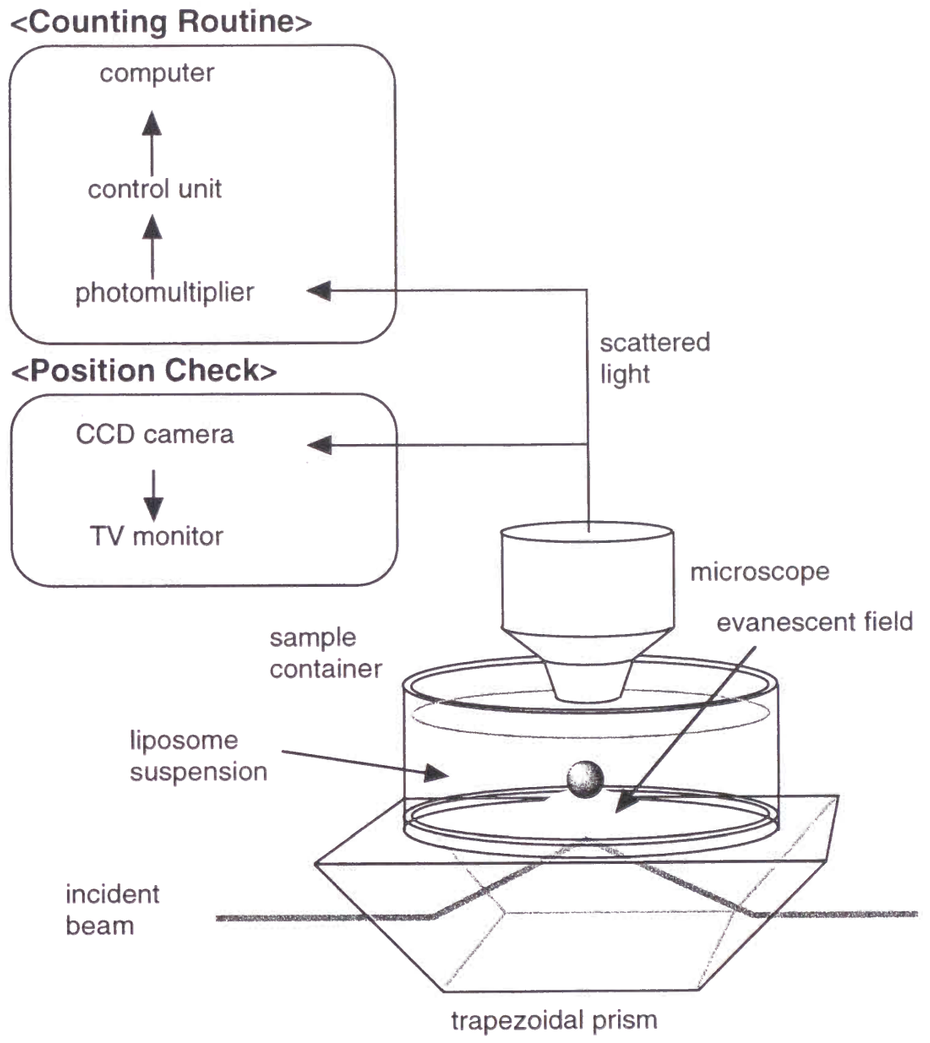

Figure 4-2 Schematic representation of the EVLSM instrument.

observation[17] etc.

Data were collected as scattering intensity in arbitrary units, as a function of time, and computed into intensity-frequency (number of observation of each intensity) histogram. The histogram can be then converted into potential energy profile as a function of the distance from interface/surface.[18] The intensity of scattered light can be translated into separation distance by using eq. (4.3) rewritten from eq. (4.1).

$$z = (\xi/2)\log(I_0/I_{EV}) \qquad (4.3)$$

In the case that the probability of finding a particle at certain distance z is represented by a Boltzmann distribution, the potential energy $V(z)$ relative to that at z_0, $V(z_0)$, is given by

$$(V(z)\text{-}V(z_0))/kT = \ln[N(I(z_0))I(z_0)/N(I(z))I(z)] \qquad (4.4)$$

where z_0 is the distance at which total potential energy is minimum, k Boltzmann's constant, T the absolute temperature of the system, and $N[I(z)]$ the observation number at $I(z)$.[5,9,19] The potential is made dimensionless by dividing by kT.

To determine absolute separation distance between the particle and the glass surface, the particle accidentally fixed on the glass surface was found and the scattering intensity of this particle was used as a standard intensity at z = 500 nm; radius of this polystyrene latex particle. The scattering intensity from fixed particle was, therefore, treated as I(500 nm), and this value, z = 500 nm, and ξ (=524 nm) were substituted for eq. (4.1). As a result, the value I_0 was calculated. After this procedure, the absolute separation distance between particle and glass surface was obtained using this I_0 value as a standard.[18,20]

4.2.3. Surface Modification.

The surface modification of glass surface was carried out by reference to the procedure of Sun et al.[21] (Fig. 4-3) 2-Acrylamido-2-methyl-1-propanesulfonic acid (AMPSA) was obtained from Tokyo Kasei (Tokyo, Japan). N, N, N', N',-tetramethylethyrenediamine (TEMED) and ammonium persulfate (APS) were purchased from Nacarai Tesque (Kyoto, Japan). 3-Methacryloxypropyl

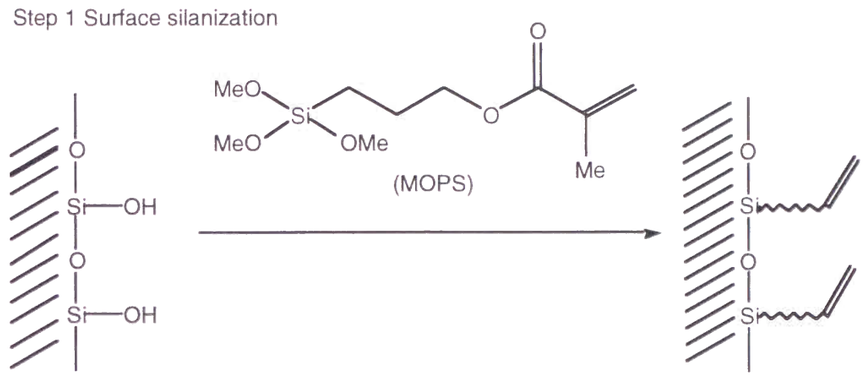

Figure 4-3 Scheme of surface modification.

trimethoxysilane (MOPS) was purchased from Chisso Co. (Chiba, Japan).

12 g of 2-Acrylamido-2-methyl-1-propanesulfonic acid (AMPSA) was dissolved in 120 ml Milli-Q grade ion-exchanged water. A concentrated NaOH solution was added to neutralize this acidic solution to pH 7.0, and brought to a total volume of 300 ml with water (NaAMPS solution). The glass plate was washed with KOH saturated ethanol for 2 hours before modification. Then the glass plate was placed in the beaker filled with saturated vapor of 3-Methacryloxypropyltrimethoxysilane (MOPS) for 2 days (step 1). After the silanization, the plate was taken out from the beaker and rinsed by water.

About 150 mg of ammonium persulfate and 150 µl of TEMED were added to NaAMPS solution, then the silanized glass plate was immersed in the mixed solution (step 2). The degree of surface modification was controlled by the reaction time. After this treatment, the glass plate was rinsed with water and dried.

4.3. Results and Discussion

4.3.1. Estimation of Character of the Modified Surface.

The existence of modified polymer layer and its homogeneity was examined by X-ray reflectivity (XR) measurement (Rigaku, Tokyo, Japan).[1,2,3,22] X-ray reflectivity is a relatively new technique for the estimation of fine structure of surface. It gives us flatness, roughness of surface and thickness in layer structure. Fig. 4-4 shows XR profile for the glass modified chemically with the procedure noted above. Kiessig fringe was observed, indicating homogeneous polymer layer on glass surface. The thickness of modification layer was calculated to be about 10 nm by the curve fitting of reflectivity curve. The surface roughness was estimated to be less than 1 nm.

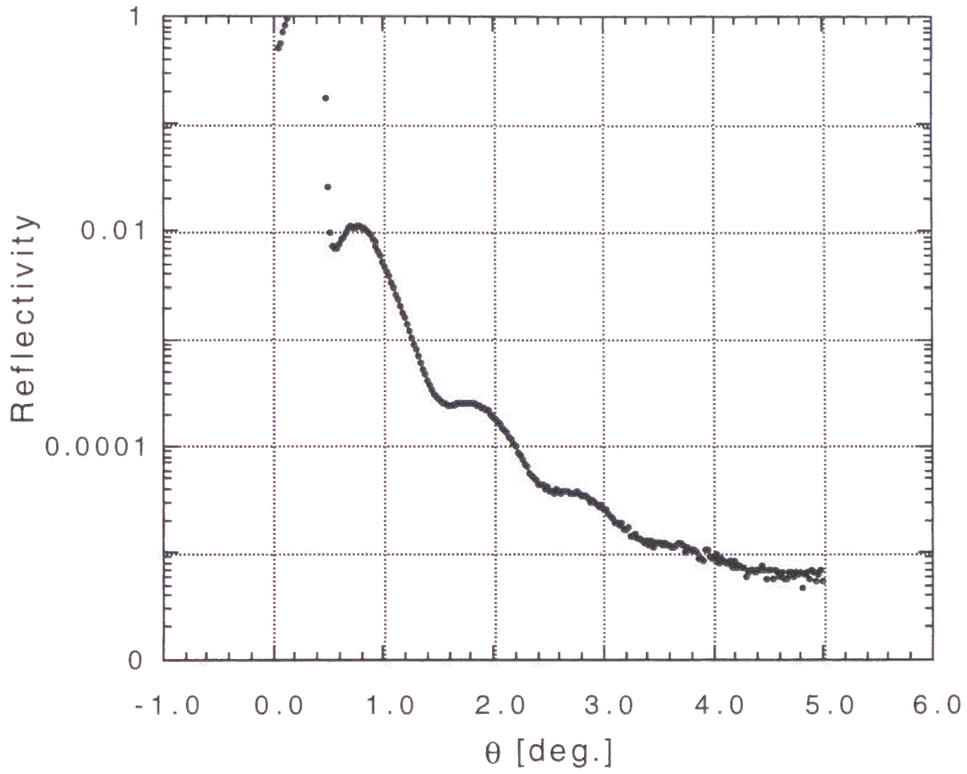

Figure 4-4 X-ray reflectivity profile for chemically modified glass.
Wave length of X-ray : 1.54Å
Reaction time : 48 hr.
ζ = -58 mV

4.3.2. Surface Zeta-Potential Measurement of the Modified Surface.

The degree of surface modification was decided by surface zeta-potential measurement. This measurement was done by a combination of electrophoretic light scattering apparatus (ELS-800, Otsuka Electronics, Osaka, Japan) and special cell unit which was developed for zeta-potential measurement of flat surface. Hydroxypropylcellulose-coated polystyrene latex (diameter : 520 nm) was used as

a probe particle for surface measurement. The absolute value of surface zeta-potential became large with increase of reaction time of Step 2. At the reaction time of Step 2 of 20 min., 5 hours, and 48 hours, the surface zeta-potential was estimated to be -7.6 mV, -36.4 mV, and -57.5 mV, respectively, while that for naked glass surface was to be -48.3 mV.

4.3.3. EVLSM Measurement.

The raw data set of EVLSM measurement (Typical example is Fig. 2-3 in Chapter 2 of this thesis.) was a time-series of scattering intensities from one particle counted by photomultiplier during one sampling time; i.e. 1 msec. in this study. The time-fluctuation of scattering intensity was directly correlated to the vibrational motion of one polystyrene latex particle in the vertical direction.

From the raw data, the histogram of the number of observation at certain scattering intensity was depicted. Fig. 4-5 is an example of histogram for this system. The horizontal axis showed scattering intensity, and the vertical is the number of observation. Since the scattering intensity corresponds to particle-wall distance as described previously, the shape of this histogram was able to be converted to the potential profile of the interaction between latex particle and glass surface by eq. (4.4).

Fig. 4-6 shows typical examples of potential profile obtained by EVLSM. The profile (a) was obtained for the system of chemically-modified glass surface (ζ = -57.5 mV), and the profile (b) was for the system of naked glass surface (ζ = -48.3 mV). The position of potential profile shifted toward the longer distance from the glass surface with increasing surface charges, and the distance of shift was about 150 nm for these examples. The amount of shift was a significant difference, although we considered that the thickness of polymer layer fixed on the glass surface had been estimated as 100 Å, i.e., 10 nm. It was adequate that these results reflected the increase of electrostatic repulsion between particles and glass surface.

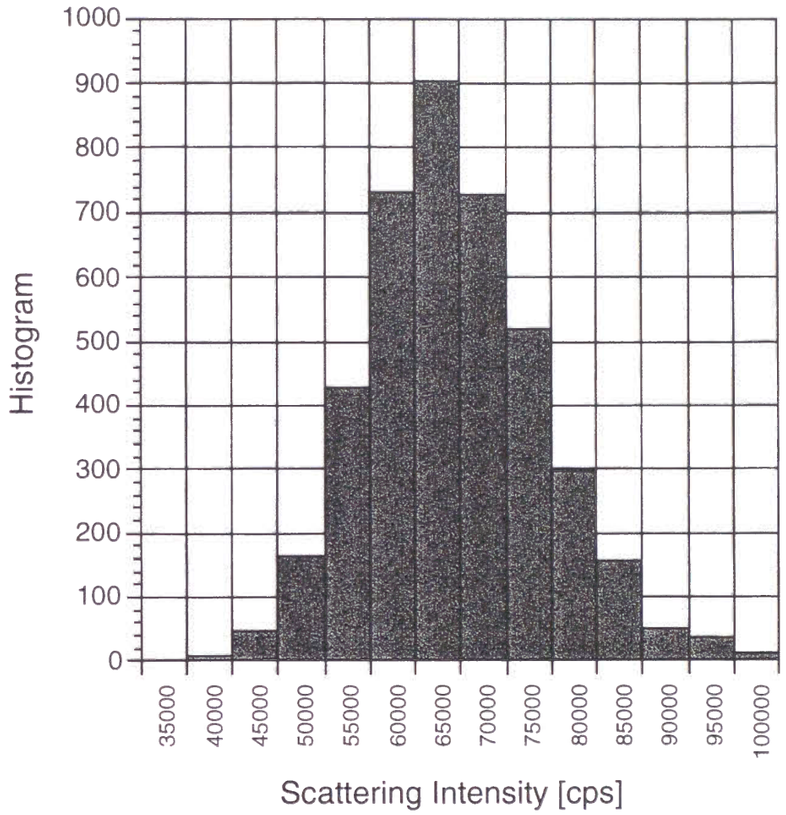

Figure 4-5 Examples of histogram obtained from EVLSM.
Particle : polystyrene latex (diameter = 1000 nm)
Surface : chemically-modofied Pyrex glass (ζ = -8 mV)
Added NaCl concentration : 0mM

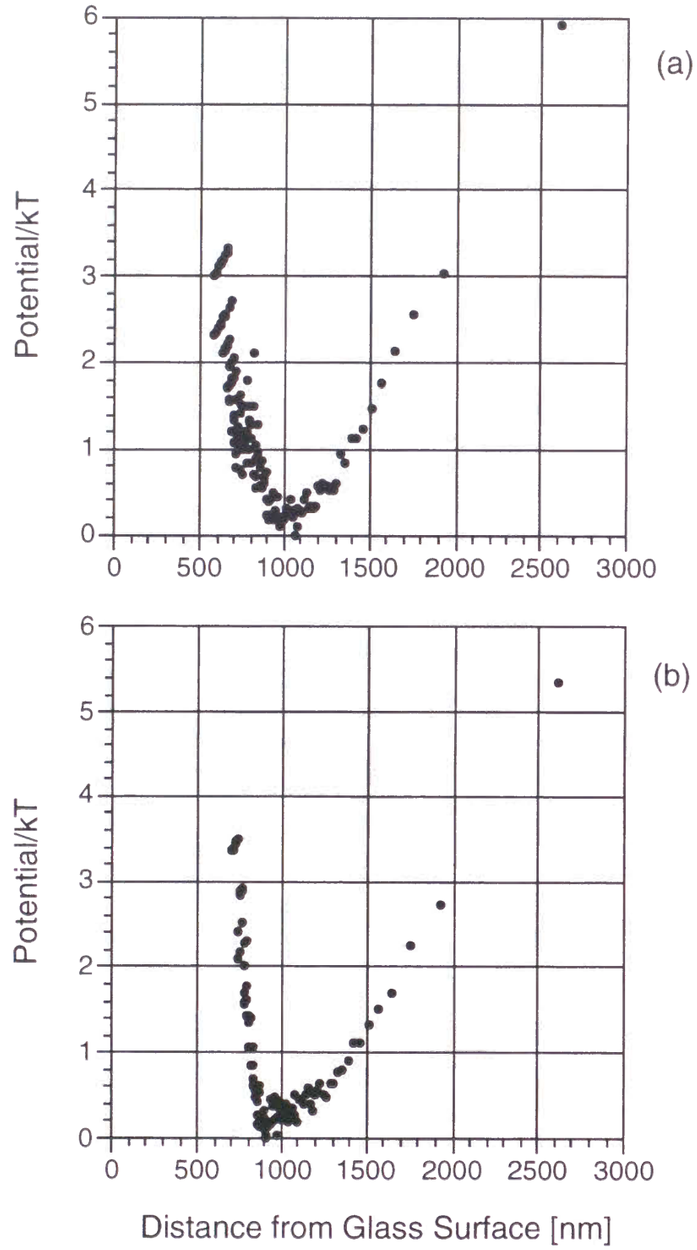

Figure 4-6 Examples of potential profiles obtained from EVLSM apparatus.
Particle : polystyrene latex (diameter = 1000 nm)
Surface : (a) chemically-modified Pyrex glass
(b) naked Pyrex glass
Added NaCl concentration : 0 mM

4.3.4. Surface Charge Dependence of Position of Interaction Potential Minimum.

The relation between the position of minimum in interaction potential profile and the zeta-potential of modified glass surface was examined. The surface zeta-potential was varied by changing reaction time of step 2 in

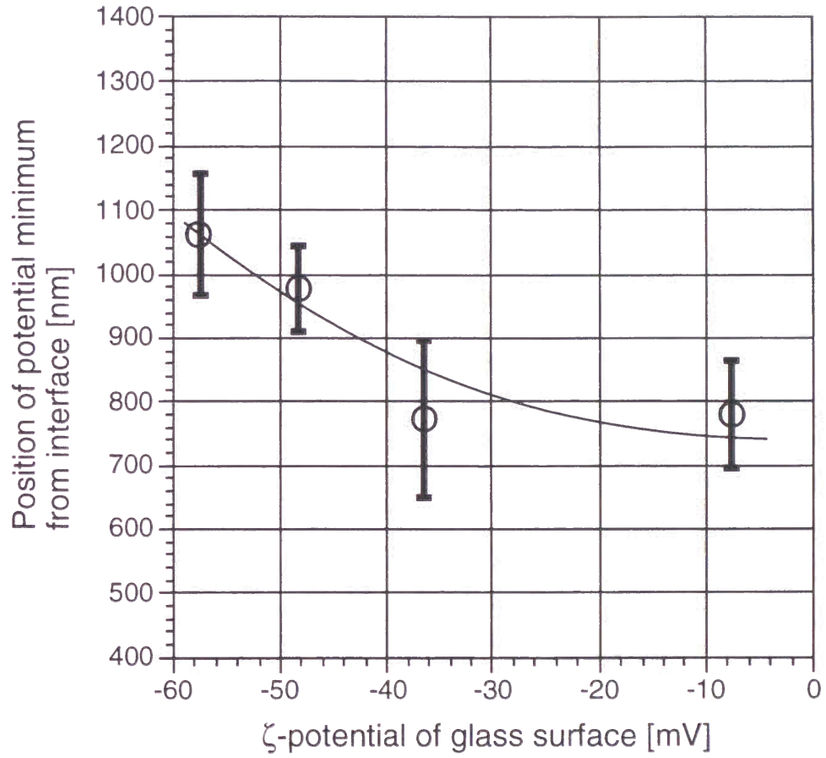

Figure 4-7 Position of potential minimum as a function of surface ζ-potential of modified glass.
Particle : polystyrene latex (diameter = 1000 nm)
Surface : naked and chemically-modified Pyrex glass
Added NaCl concentration : 0mM

modification procedure we adopted. The position of interaction potential minimum was calculated from potential profile obtained from EVLSM measurements. The result was shown in Fig. 4-7. The horizontal axis was zeta-potential of glass surface, the vertical the position of potential minimum from glass surface. The error bar showed standard error. The position of minimum shifted toward larger distance from the interface with increasing the absolute value of zeta-potential of the glass surface. At the value was about -58 mV the position of minimum was 1060 nm, and it was 780 nm at the value about -8 mV. The increase of the absolute value of zeta-potential of glass surface can be attributed to the increase of surface negative charges on the glass surface. The electrostatic repulsion between negative charges on the surface of particle and of glass wall became large with increasing surface charges. Meanwhile, the gravity did not vary with modification of glass surface. Therefore, the position of potential well which is formed by particle - surface electrostatic repulsion and the gravity moved toward longer distance from the glass surface.

4.3.5. Ionic Strength Dependence of Position of Interaction Potential Minimum.

The position of potential minimum was estimated as a function of the concentration of NaCl added in the colloidal dispersion (Fig. 4-8). The left one is obtained for naked glass surface, and the right one is for chemically-modified glass. In both cases, the position of potential minimum shows the similar tendency. Higher the concentration of NaCl, closer the position to the surface. At the condition of relatively high NaCl concentration, the electrostatic interaction between the surface of colloidal particle and naked/chemically-modified glass was shielded. Hence, the electrostatic repulsion between particle and glass surface reduced, and the position of interaction potential well came closer to the glass surface.

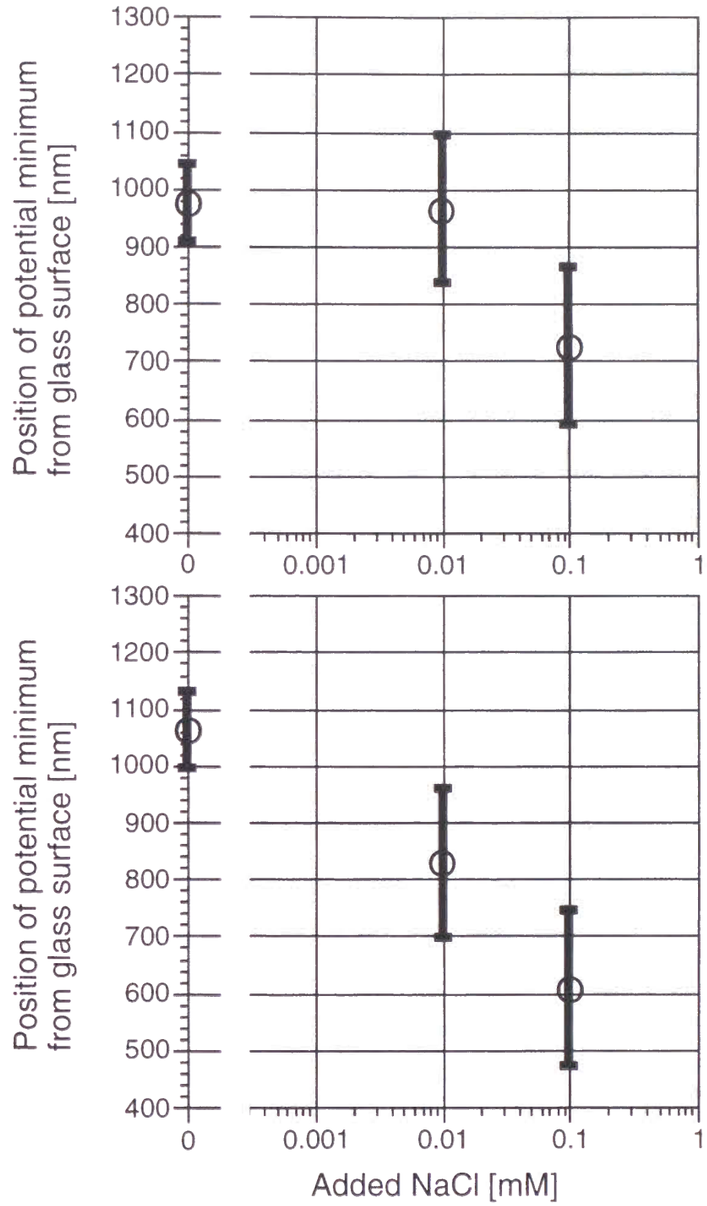

Figure 4-8 Position of potential minimum as a function of added NaCl concentration in the system.
Particle : polystyrene latex (diameter = 1000 nm)
Surface : naked and chemically-modified Pyrex glass
Added NaCl concentration : 0mM, 0.01mM, 0.1mM

4.3.6. Advantage of EVLSM and Comparison with other Techniques.

Although some unclear points for EVLSM technique have been pointed out, such as the relatively larger particle size compared to the wave length and the penetration depth, EVLSM technique has large possibility of application.

One possibility for application of EVLSM may be an estimation of external forces. In this study, the external force was gravity. This can be another force such as electric field, magnetic field etc., and these forces can be evaluated by EVLSM, if necessary. In the present polystyrene latex particle-glass system, the electrostatic interaction was detected by EVLSM since it is the dominant factor. Other interaction should be detected, if it is dominant, such as hydrogen-bonding, antigen-antibody interaction, especially in biological systems.

Recently, AFM is extensively applied to measure particle-surface forces in addition to surface imaging.[23] As already described, it is necessary to glue one colloidal particle to the cantilever as a tip and measured the force directly. In EVLSM, the interaction potential can be estimated ***without*** fixing particle; we can measure interaction for the particle in ***free*** state. This is a great advantage of EVLSM compared to the AFM since it has been gradually clarified that the dynamic properties of colloidal particle and/or counterions play an important role in the electro "static" interaction.[24]

4.4. Conclusion

It has shown that EVLSM is a powerful tool to estimate electrostatic forces between a colloidal particle and a flat surface. The minimum position of interaction potential under gravity between polystyrene latex particle of diameter 1000 nm and glass flat plate where sulfonate groups were fixed chemically in dispersion were estimated as functions of surface zeta-potential of glass and of ionic strength.

The position of potential minimum of particle - wall interaction shifted toward larger distance from glass surface, as the absolute value of surface zeta-potential became large with surface modification. When electrolytes were added to the colloidal system, the position of the interaction potential well became closer to the naked / chemically-modified glass surface. These results can be accounted to be caused by changes of electrostatic interaction between particle and surface under constant gravity.

It can be said that EVLSM becomes a more important method for the interfacial study and the extensive utilization of EVLSM will be done in near future. The next step may be more quantitative discussion with colloidal interaction theories.

References

(1) Yamaoka, H.; Matsuoka, H.; Kago, K.; Endo, H.; Eckelt, J. *Physica B* in press.

(2) Matsuoka, H.; Yamaoka, H. *Proceedings of Risø International Symposium Material Science* **1997**, *18*, 437.

(3) Kago, K.; Matsuoka, H.; Endo, H.; Eckelt, J.; Yamaoka, H. *Supramol. Sci.* submitted.

(4) Kago, K.; Endo, H.; Matsuoka, H.; Yamaoka, H.; Hamaya, N.; Sasaki, S.; Mori, T. *J. Synch. Rad.* submitted.

(5) Tanimoto, S.; Matsuoka, H.; Yamaoka, H. *Colloid Polym. Sci.* **1995**, *273*, 1201.

(6) For example, Braithwaite, G. J. C.; Howe, A.; Luckham, P. F. *Langmuir* **1996**, *12*, 4224.

(7) Tanimoto, S.; Kitano, H. *Colloids and Surfaces B* **1995**, *4*, 259.

(8) Tanimoto, S.; Kitano, H. *Langmuir* **1993**, *9*, 1315.

(9) Prieve, D. C.; Frej, N. A. *Langmuir* **1990**, *6*, 396.

(10) Tanimoto, S.; Takahashi, K.; Matsuoka, H.; Yamaoka, H. *Colloids and Surfaces*, submitted.

(11) Bike, S. G.; Prieve, D. C. *Int. J. Multiphase Flow* **1990**, *16*, 727.

(12) Prieve, D. C.; Bike, S. G.; Frej, N. A. *Faraday Discuss. Chem. Soc.* **1990**, *90*, 209.

(13) Walz, J. Y.; Prieve, D. C. *Langmuir* **1992**, *8*, 3073.

(14) Harrick, N. J. "Internal Reflection Spectroscopy", Interscience, New York, (1967)

(15) Newton, I. (1952) Opticks, Dover, New York

(16) Hunter, R. J. "Zeta Potential in Colloid Science", Academic, London, Chap. 7, (1988)

(17) Ito, K.; Nakamura, H.; Yoshida, H.; Ise, N. *J. Amer. Chem. Soc.* **1988**, *110*, 6995.

(18) Flicker, S. G.; Tipa, J. L.; Bike, S. G. *J. Coll. Int. Sci.* **1993**, *158*, 317.

(19) Flicker, S. G.; Bike, S. G. *Langmuir* **1993**, *9*, 257.

(20) Tanimoto, S.; Yamauchi, H.; Matsuoka, H.; Yamaoka, H. *Polymer Preprints* **1997**, *46*, 894.

(21) Sun, P.; Landman, A.; Barker, G. E.; Hartwick, R. A. *Journal of Chromatography A* **1994**, *685*, 303.

(22) Yamaoka, H.; Matsuoka, H.; Kago, K.; Eckelt, J.; Endo, H. *Langmuir* in press.

(23) Ducker, W.; Senden, T.; Pashley, R. *Langmuir* **1992**, *8*, 1831.

(24) Matsuoka, H.; Harada, T.; Kago, K.; Yamaoka, H. *Langmuir* **1996**, *12*, 5588.

Part II

Chapter 5

Binding Kinetics of Antibodies to Antigens on Polymer Surfaces as Studied by the Evanescent Wave Fluorescence Method

Abstract

Binding process of an antibody (anti-human serum albumin-immunoglobulin G) labeled with fluorescein (FITC-anti-HSA-IgG) to an antigen (HSA) bound to polymer surfaces was followed by the multiple internal reflection fluorescence (MIRF) method. The antigen (HSA) was adsorbed strongly onto hydrophobic polymer surfaces (poly(methyl methacrylate) (PMMA)), and the protein adsorbed was scarcely removed by rinsing with a buffer solution. The initial rate of the binding of FITC-anti-HSA-IgG to the antigen on the polymer surface was very large (about 10 % of the diffusion-controlled association at the most), whereas there was no binding of the antibody to the surface modified with ovalbumin (OVA). The effects of surface density of the antigen on the binding rate and the amount of antibody bound were examined.

5.1. Introduction

In spite of the importance of analyses of specific binding processes between a protein and a complementary ligand located on solid surfaces, [1,2] only a few studies concerning binding kinetics have been carried out because of its experimental difficulties.

To avoid disturbing factors in evaluating the kinetics of specific protein binding (in the column method, for example, void volume, pore size, and flow rate affect the protein binding), [3-6] the binding on flat surfaces is suitable though the sensitivity of the detector has to be very high. Internal reflection spectroscopy, which adopts the evanescent wave generated by the total internal reflection, is useful to sensitively detect target molecules within several tens of nanometers from the flat surface.

Recently the internal reflection method has been applied to detect proteins adsorbed onto solid surfaces and to follow immunological reaction. In these studies, the adsorption of proteins onto a flow cell was examined, though the kinetic analysis of the processes of protein binding was complicated.

In this thesis, the very initial stage (within several seconds after the onset of the binding) of the specific binding of an antibody (anti-human serum albumin-immunoglobulin G) onto a flat surface of poly (methyl methacrylate) (PMMA) modified with an antigen (human serum albumin) was followed by the multiple internal reflection fluorescence (MIRF) method using a non-flow cell system. Figure 5-1 shows the system studied in this chapter.

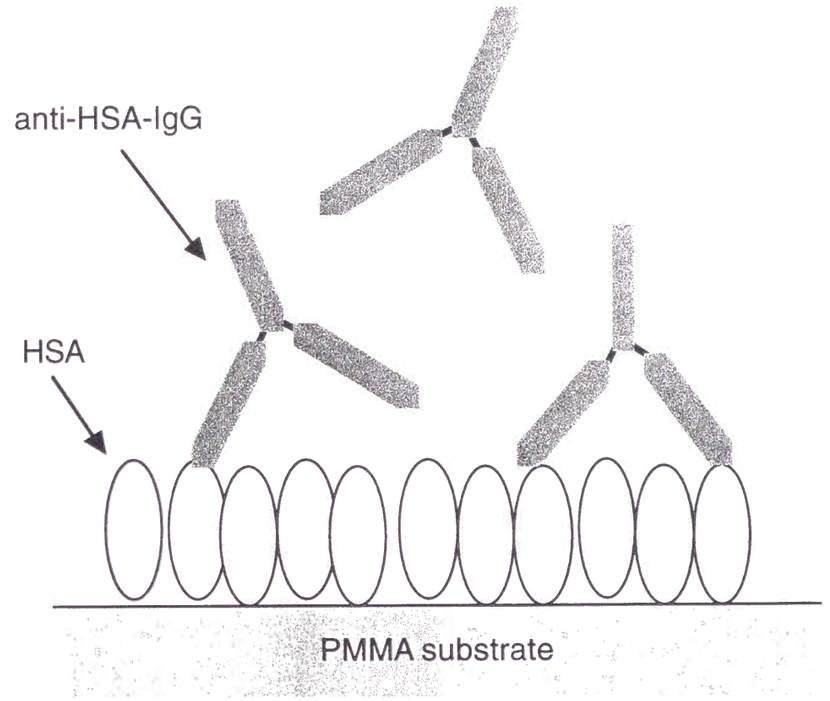

Figure 5-1 The image of the system used in this chapter. The antibodies is aproaching to HSA-modified surface.

5.2. Experimental Section

5.2.1. Materials.

Human serum albumin (HSA, fatty acid free, A3782) was purchased from Sigma (St.Louis, MO). Ovalbumin (OVA) was from Seikagaku Kogyo Co. (Tokyo, Japan). An antibody, anti-HSA-IgG modified with FITC (FITC-anti-HSA-IgG), was

from MBL (Nagoya, Japan). The size of the antibody was confirmed to be homogeneous by gel permeation chromatography (GPC) using a Sephadex G-150 column (2 i.d. x 30 cm). Fluorescein isothiocyanate (FITC, Art 24546, Aldrich, Milwaukee, WI) was used to label the proteins (HSA and OVA). Labeling was carried out in a carbonate buffer (pH 9.5, 0.05 M) for 2 hr. at 5°C.[14] Free FITC was separated from fluorescein bound to the protein by GPC using a Sephadex G-25 column (2 i.d. x 30 cm) with a phosphate buffer (pH 7.0, 10 mM) as a mobile phase. The labeled protein was fractionated by the number of fluorescein groups per protein molecule (F/P ratio) by using ion-exchange chromatography (DEAE-cellulose, 2 i.d. x 30 cm).[14] The number of fluorescein groups per antibody molecule (F/P ratio) was determined by comparing the absorbance at 490 nm with the absorbance at 280 nm obtained from a UV spectrophotometer (U-3400; Hitachi, Tokyo, Japan). HSA of F/P=1.4, OVA of F/P=0.4 and anti-HSA-IgG of F/P=0.8 were used in this chapter.

5.2.2. Apparatus for MIRF.

The details of the MIRF apparatus[12] used in this work (Figure 5-2) were described below. The light source was an argon laser (488 nm, 10 mW, LAI2223, Toshiba Electronics, Tokyo, Japan). The excitation beam was introduced into the wave guide through the prism, hit the interface between the wave guide and sample solution at an angle of 80°, and was reflected at the interface. Consequently, the evanescent wave was generated and penetrated into the sample solution beyond the interface. The penetration depth (dp) of the evanescent wave was 1500 Å. The excitation beam was emitted inside of the wave guide with multiple reflections.

When a FITC-protein is bound to the surface of the wave guide, a fluorescein group is excited by the evanescent wave and emits fluorescence. The fluorescence moves back to the opposite direction of the excitation beam and

comes out the wave guide through the prism. The fluorescence is separated from the excitation beam using a dichroic mirror and a cut filter and is finally detected by a photomultiplier (R-1547, Hamamatsu Photonics, Hamamatsu, Japan).

The wave guide with prisms is made of poly(methyl methacrylate) (PMMA) and used only once. The wave guide has an intrinsic background signal due to fluorescent impurities within the wave guide.[15] The relative fluorescence intensity corresponding to the background signal of the wave guides used here was 15 ± 1, and we could assume that optical properties of the wave guides were constant. The surface area of the wave guide with which the sample solution can

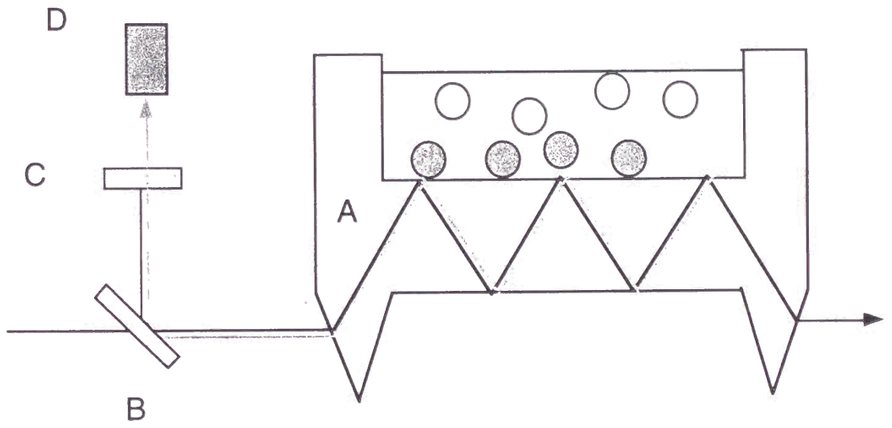

Figure 5-2 Schematic of the MIRF method.
Plain line, excitation beam; gray line, fluorescence; open circle, FITC-protein (without excitation); closed circle, FITC-protein (excited); A, optical wave guide with prisms; B, dichroic mirror; C, cut filter; D, detector.

be in contact is 4 cm^2 (1 x 4 cm). A cuvette consists of the wave guide and a cover (stainless steel) with ports for an injection of the sample solutions. The total thickness of the cell is about 0.5 mm, and the total cell volume including the injection ports is about 0.25 ml.

The fluorescence signal through the cut filter is detected by the photomultiplier, and the fluorescence intensity was integrated for 1 sec. A monochrometer reference is also detected, and the difference between the intensities of the reference signal and the fluorescence signal is calculated with a microcomputer (J-3100 GT, Toshiba Electronics, Tokyo, Japan).

5.2.3. Assay Procedure.

The wave guide of the MIRF was washed with a soak solution, rinsed with deionized water, and treated with a halogenated hydrocarbon, Daiflon S-3 (Daikin Industries, Osaka, Japan) before use. The sample solutions were prepared with a phosphate buffer (pH 7.0, 10 mM). The cell was incubated with the buffer for several minutes beforehand, and within 20 s after a removal of the buffer solution, the sample solution (0.25 ml) was injected into the cell by an autopipetter (Microelectropette, Matrix Technologies, Lowell, MA) to keep the injection speed constant. In the experiments of specific binding of anti-HSA-IgG to the cell, the cell was incubated with the solution of proteins (HSA or OVA) mostly for 3 h, and after washing the cell with the buffer, the solution of the anti-HSA-IgG was injected (within 20 s after the removal of the buffer).

5.2.4. Calibration Experiment.

For calibration experiments, the surface concentration of proteins on the MIRF cell was determined as follows: the protein solution of various concentrations (10-100 mg/ml) was injected into the MIRF cell. The concentration of the protein solution injected and that recovered from the cell

600 s after the injection were immediately estimated from fluorescence intensity at 520 nm (excitation 480 nm) using a fluorescence spectrophotometer (F-410, Hitachi, Tokyo, Japan). The decrease in the fluorescence intensity of the solution after the binding experiments was 4.5 - 15.6 % of that of the initial solution. The surface concentration of the protein (C_s) could be determined from the difference of the concentrations before and after the injection.

5.3. Results and Discussion

5.3.1. Adsorption of Proteins to Cuvettes.

At first, we examined the nonspecific adsorption of proteins modified with FITC onto PMMA cuvette. After injection of the FITC-protein solution into the naked cuvette, there was a rapid increase in fluorescence intensity, and the intensity leveled off within 300 sec. Six hundred seconds after the injection of HSA solution, the solution above the cuvette was replaced by a buffer solution. There was, however, no significant decrease in fluorescence intensity, which showed no exchange of proteins between the bulk solution and the polymer surface, and at the same time, the effect of background signal corresponding to the FITC-proteins in the bulk solution on the detected fluorescence intensity was negligible.

The amount of proteins bound to the surface (C_s) and the increase in fluorescence intensity showed a linear relationship.[12] The initial binding rate $(dC_s/dt)_0$ obtained by the initial increase in fluorescence intensity increased linearly with a concentration of proteins in the solution injected, too. The ratio (R) of the experimental binding rate to the theoretical value for a diffusion-controlled binding, $(dC_s/dt)_{theor}$ (given by eq (5.1)),[16] was estimated by eq (5.2).

$$(dC_S/dt)_{theor} = C_0(D/\pi t)^{0.5} \qquad (5.1)$$

$$R = (dC_S/dt)_0 \,/\, (dC_S/dt)_{theor} \qquad (5.2)$$

where C_0 and D are the concentration of the FITC-protein and the diffusion coefficient of the protein,[17] respectively. The obtained R values were 0.9 (anti-HSA-IgG), 0.7 (HSA), and 0.6 (OVA).

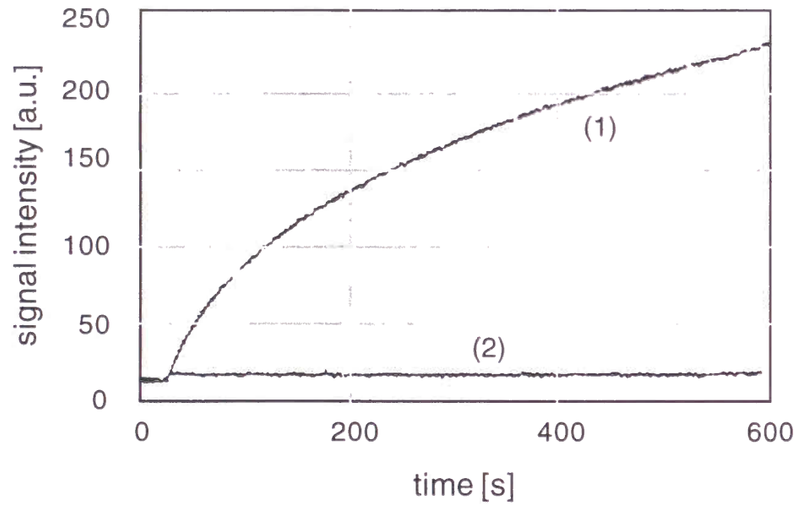

Figure 5-3 Typical profile of the increase in fluorescence intensity after injection of the solution of FITC-anti-HSA-IgG into the PMMA cuvette.
(1) the cuvette had been incubated with a HSA solution;
(2) the cuvette had been incubated with a OVA solution.

5.3.2. Binding of Antibodies to Antigens on Polymer Surfaces.

Next we examined the binding of anti-HSA-IgG to the polymer surface modified with proteins (Fig. 5-3). When the surface was covered with HSA, IgG bound quickly (curve 1).

The very small but rapid increase in fluorescence intensity at the beginning of curve 2 can be ascribed to two factors; (1) the nonspecific binding of the antibody to the polymer surface uncovered, and (2) the background signal.

When we varied the conditions of incubation ([HSA]=1 mg/ml for 20 min., 5 mg/ml for 3 h), the R value changed. By the incubation of the cuvette with a solution of HSA (5 mg/ml) for 3 h, the cuvette was fully covered with HSA. We, therefore, used these conditions (incubation of the cuvette with a protein solution (5 mg/ml) for 3 h) in this experiment. Even under these incubation conditions, however, there was an increase of the same degree in fluorescence intensity as that of the curve 2 in Fig. 5-3. Consequently, the contribution of nonspecific binding to the initial rapid increase in fluorescence intensity can be neglected, and we attributed the increase to the background signal.

To confirm the contribution of the background signal to the total MIRF signal, we injected the FITC solution, which had the same fluorescence intensity to that of the antibody solution, into the naked cuvette. The increase in fluorescence intensity after injection of the FITC solution was the same as that observed by the injection of the antibody solution to the cuvette which had been covered with OVA molecules. Therefore, the increase in fluorescence intensity (curve 2 in Fig. 5-3) was concluded to be due to the background signal corresponding to the FITC-anti-HSA-IgG in the bulk solution.

The reason for such a discrepancy (the negligible effect of background signal in the nonspecific binding (section 5.3.1) and the considerable effect in the specific binding (this section)) is due to the difference in the binding rate: Nonspecific binding of the antibody to the naked polymer surface is very rapid,

whereas the immunological binding to the surface modified with the antigens is relatively much slower. Therefore, the initial increase by the background signal just after the injection of the solution containing fluorophores was not negligible in the latter case. We, therefore, corrected the observed increase in fluorescence intensity by subtracting the effect of the background signal in this immunological reaction system.

When the cuvette was incubated with a HSA solution (5 mg/ml) for 3 hr., the R value for the binding of anti-HSA-IgG to HSA adsorbed on the cuvette was 0.07, which is about 1/10 of the rate for the nonspecific binding of IgG to the naked cuvette. The rate constant for the binding of anti-HSA-IgG with HSA was reported to 1.9 x 10^6 $M^{-1}s^{-1}$ at pH 8.0 and 25 °C.[18] The rate constants for other immunological systems including proteins as antigens are 1.0 x 10^6 $M^{-1}s^{-1}$ (OVA and anti-OVA-antibody) [19] and 1.0 x 10^6 $M^{-1}s^{-1}$ (cytochrome C and anti-cytochrome C).[20] The second-order rate constant for a diffusion-controlled association between particles a and b is given by eq. (5.3).[21,22]

$$k_2=4\pi N_A(D_a+D_b)R_{ab}/1000 \qquad (5.3)$$

where N_A, D_a, and R_{ab} are the Avogadro number, the diffusion coefficient of particle a, and the closest distance between centers of the particles a and b, respectively. The theoretical rate constant (k_2) for a diffusion-controlled association of these antigen proteins with corresponding antibodies in solution are on the order of 10^{10} $M^{-1}s^{-1}$, and the R value for these immunological systems would be around 10^{-4}.

To realize an association of an antigen with an antibody, a binding site of the antigen has to be correctly oriented to a binding site of the antibody at the collision. In the binding of an antibody with an antigen, such a steric effect largely reduces percents of effective collision for an association. The reason of the big

difference in the R values for the solution system (R~10^{-4}) and the liquid-solid interface system (R~10^{-1}), however, is not still clear.

5.3.3. Effect of Surface Density of Antigens on the Rate of Specific Binding.

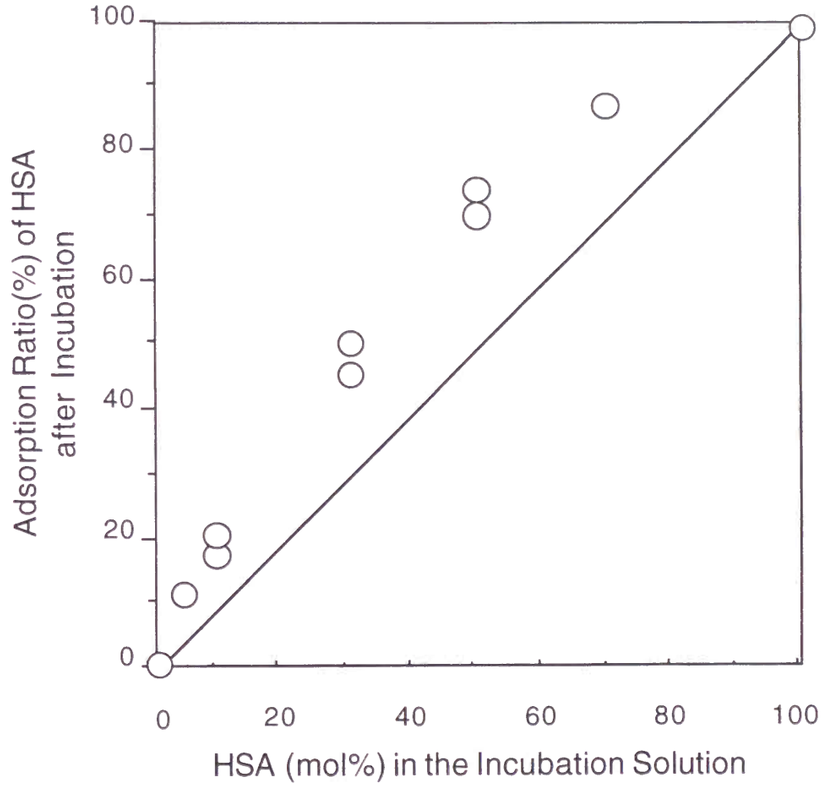

Figure 5-4 Effect of HSA percentage in the incubation solution on the percent of HSA adsorbed on the surface of the cuvette.

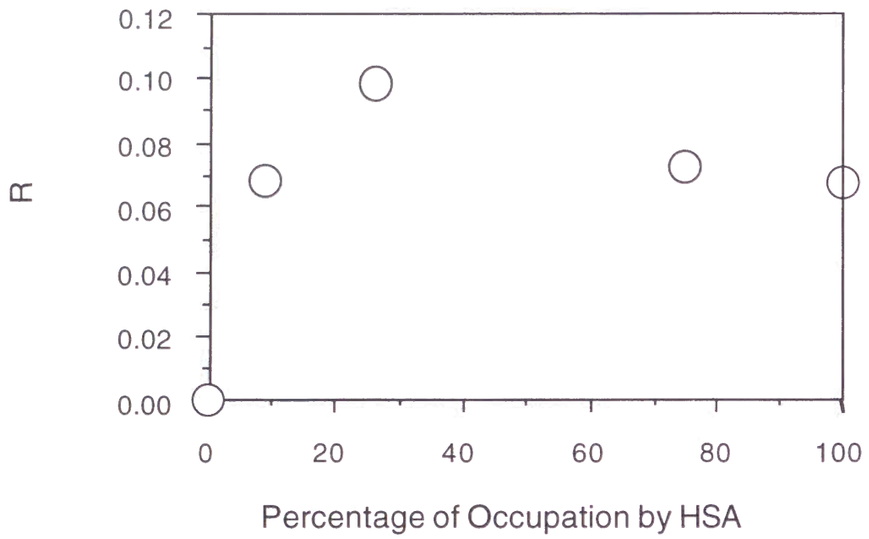

Figure. 5-5 R value at various percentages of occupation by HSA on the surface of the cuvette.

When the ratio of HSA and OVA in the incubation solution was changed, we could modify the surface of the cuvette with HSA and OVA, at various ratios (Fig. 5-4). Fig. 5-4 also suggested that the binding rate of HSA is larger than that of OVA, which is consistent with the data shown in section 5.3.1. Fig. 5-5 shows the *R* value for various HSA/OVA ratios on the surface of the cuvette. When the percent of occupation by HSA on the surface was zero, there was no binding, whereas in the presence of HSA of 8 %, the *R* value was 0.07, and at 25 % the *R* value reached the maximum (0.10), and then gradually decreased. the decrease in *R* value might be due to the rearrangement of HSA molecules on the polymer

surface at higher surface concentrations.

In addition, we measured the MIRF signal 600 sec. after onset of the binding experiment at various percents of occupation by HSA (Fig. 5-6). Similarly to the tendency of *R* values, the amount of antibody bound increased with the increase in the percent of HSA on the cuvette surface and then leveled off.

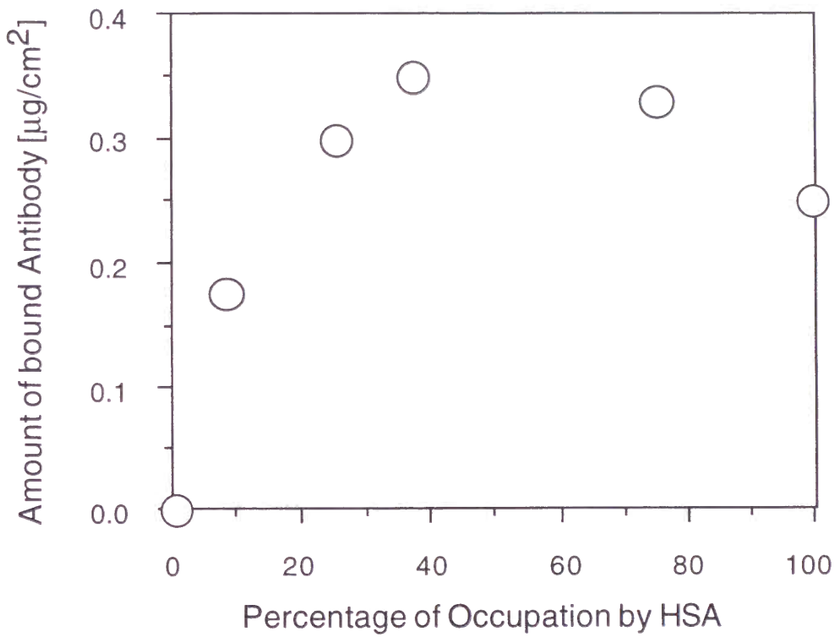

Figure 5-6 Amount of antibody bound to the surface of the cuvette which was modified with HSA at various percentages. [FITC-anti-HSA-IgG] = 50 μg/ml.

The MIRF technique examined here would be very useful for various

association systems in the solid-liquid interface.

References

(1) Andrade, J. D.; Hlady, V. *Adv. Polym. Sci.* **1986**, *79*, 1.

(2) Mosbach,K., Ed. Methods in Enzymology; Academic Press: New York, 1987; Vol. 135.

(3) Tashiro, Y.; Kataoka, K.; Sakurai, Y. *J. Colloid Interface Sci.* **1990**, *66*, 140.

(4) Kitano, H.; Nakamura, K.; Hirai, Y.; Kaku, T.; Ise, N. *Biotechnol. Fioeng.* **1988**, *31*, 547.

(5) Nakamura, K.; Hirai, Y.; Kitano, H.; Ise, N. *Biotechnol. Bioeng.* **1987**, *30*, 216.

(6) Hasegawa, M.; Kitano, H. *Biotechnol. Bioeng.* **1991**, *37*, 608.

(7) Hirschfeld, T. *Can. Spectrosc.* **1965**, *10*, 128.

(8) Lok, B. K.; Cheng, Y.; Robertson, C. R. *J. Colloid Interface Sci.* **1983**, *91*, 87.

(9) Hlady, V.; Reinecke, D. R.; Andrade, J. D. *J. Colloid Interface Sci.* **1986**, *111*, 555.

(10) Beissinger, R. L.; Leonard, E. F. *ASAIO J.* **1980**, *3*, 160.

(11) Sutherland, R. M.; Dähne, C.; Place, J. F.; Ringrose, A. S. *Clin. Chem.* **1984**, *30*, 1533.

(12) Hasegawa, M.; Kitano, H. *Langmuir* **1992**, *8*, 1582.

(13) Harrick, N. J.; Loeb, G. I. *Anal. Chem.* **1973**, *45*, 687.

(14) Maeda, H.; Ishida, N.; Kawauchi, H.; Tuzimura, K. *J. Biochemistry* **1969**, *65*, 777.

(15) Rockhold, S. A.; Quinn, R. D.; Van Wgenen, R. A.; Andrade, J. D.; Reichert, M. *J. Electroanal. Chem.* **1983**, *150*, 261.

(16) MacRitche, F. *Adv. Protein Chem.* **1978**, *32*, 283.

(17) Fasman, G. D., Ed. Handbook of Biochemistry and Molecular Biology, 3rd ed.; CRC Press: Cleveland, OH, 1976; Vols. I-III.

(18) Kitano, H.; Iwai, S.; Okubo, T.; Ise, N. *J. Am. Chem. Soc.* **1987**, *109*, 7608.

(19) Levison, S. A.; Jancsi, A. N.; Dandliker, W. B. *Bichem. Biophys. Res. Commun.* **1968**, *33*, 942.

(20) Noble, R. W.; Reichlin, M.;Gibson, Q. H. *J. Biol. Chem.* **1969**, *244*, 2403.

(21) Bird, R. B.; Stewart, W.B.; Lightfoot, E. N. Transport Phenomena; Wiley: New York, 1960; p 780.

(22) Kitano, H.; Iwai, S.; Ise, N.; Okubo, T. *J. Am. Chem. Soc.* **1987**, *109*, 6641.

Chapter 6

Binding Kinetics of Antibody to Hapten-doped Lipid Monolayers as Studied by the Evanescent Wave Fluorescence Method

Abstract

Binding processes of an antibody (anti-dinitrophenyl(DNP)-immunoglobulin E) labeled with fluorescein groups (FITC-anti-DNP-IgE) to a hapten-doped lipid monolayer were followed by the multiple internal reflection fluorescence (MIRF) method, because of its usefulness in detecting the adsorption of binding of target molecules at the interface. The hapten-doped lipids used in this work were dinitrophenyl-phosphatidylethanolamine (DNP-DPPE) and dinitrophenyl-aminocaproyl-phosphatidyl-ethanolamine (DNP-cap-DPPE), and a monolayer containing the hapten-doped lipid was deposited on a poly(methyl methacrylate) cuvette by using the Langmuir-Blodgett technique.

The fluorescence signal increased with the binding of the antibodies, and the initial binding rate was calculated from the slope of the fluorescence signal curve. The initial rate of the binding of FITC-anti-DNP-IgE to the hapten on the lipid monolayer surface increased at a low surface density of haptens in the lipid monolayer, and leveled off at a moderate-to-high hapten density. The effect of spacer length between the hapten group and the lipid layer on the binding rate was also examined. It was confirmed that a long spacer promoted the access of antibodies to the haptens.

6.1. Introduction

The analysis of specific binding processes between a protein and its complementary ligand located on lipid surfaces is very important in various fields: medical chemistry, biochemistry and bioengineering, for example. Specific binding between an antigen and an antibody is one of the typical molecular recognition reactions *in vivo* . It has been clarified that some immunological reactions occur on the membrane surface of T cells.[1] However, an understanding of the detailed mechanism of various immunological phenomena in cell systems will not be easily achieved in the near future, as long as primitive observation of the interactions among the immune cells such as cytotoxic cells or macrophages mixed *in vitro* are carried out.

Kinetic studies of antigen-antibody reactions in solution using the stopped-flow technique have been already carried out as the first step of kinetic analysis of immunological reactions.[2] In living systems, however, antigens are fixed on the cell membranes in most cases, and an antibody recognizes the antigen at the cell surface and binds to it. Therefore, it is highly probable that the binding ability of the antibody is affected by the situation of the antigen at the membrane surface. However, very few studies of surface immunological kinetics have been performed,[3,4] because the method of observing the initial step of the specific antigen-antibody binding reaction at the interface has not yet been established.

To avoid disturbing factors in the evaluation of the kinetics of specific protein binding (in the column method, for example, void volume, pore size and flow rate unavoidably affect the protein binding),[5-8] binding onto flat surfaces is a quite suitable system for study, although the sensitivity of the detector has to be high.

Multiple internal reflection fluorescence (MIRF) method, which is based on the property of an evanescent wave generated by total internal reflection, is

useful for sensitively detecting target molecules within several tens of nanometers of the flat surface[9]. Recently, the internal reflection method has been applied to detect proteins adsorbed onto solid surfaces,[10-12] and to follow immunological surface reactions.[13] In these studies, the binding of proteins onto a quartz flow cell was examined because of high optical purity of the quartz, although the kinetics analysis of the binding processes of proteins is complicated

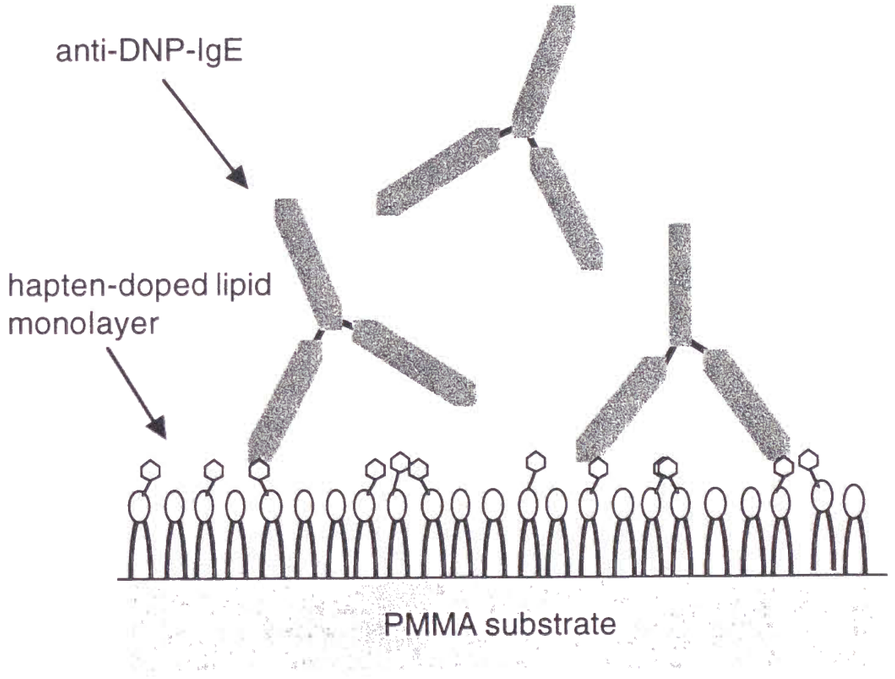

Figure 6-1 The image of the system used in this chapter.
The antibodies is aproaching to hapten-doped lipid monolayer.

in a flow system. Taking these facts into consideration, a disposable cell made of poly(methyl methacrylate) (PMMA) has been used in our group for carrying out internal reflection spectroscopy.[14-16]

In this report, the initial stage of the specific binding of an antibody onto a flat surface of hapten doped lipid monolayer was followed by using the multiple internal reflection fluorescence (MIRF) method. The image of system studied in this chapter is shown in Fig. 6-1.

6.2. Experimental Section

6.2.1. MIRF Apparatus.

The details of the MIRF apparatus used in this study (Fig. 6-2) were given in the previous chapter and our publications.[14-16] The special cell, with waveguide and prisms, is made of poly(methyl methacrylate) (PMMA) and was used only once. The cell was washed with deionized water and treated with a halogenated hydrocarbon, 1,1,2-trichloro-2,2,1-trifluoroethane (Daiflon S-3; Daikin Industries Osaka, Japan), before the deposition of the lipid monolayers. During the measurements, a stainless-steel cover is attached to the cell, the size of which is 10 mm x 40 mm x 1.5 mm. Each measurement requires only 250 µl of sample solution. The incident light was an argon ion laser (488 nm, 10 mW; model LA12223; Toshiba Electronics, Tokyo, Japan). The incident beam through the prism and waveguide generates an evanescent wave on total reflection at the interface between the waveguide and the sample solution.

The evanescent wave passes into the sample solution across the interface and excites the fluorescent substances that are bound to the target colloidal particles in the near neighborhood of the interface. The emitted fluorescence travels back into the waveguide, retraces the path of the beam and passes out

through the prism. The fluorescence is separated from the incident beam with a dichroic mirror and a cut filter (R515; Schott), and is finally detected by use of a photomultiplier (R-1547, Hamamatsu Photonics, Hamamatsu, Japan). The laser beam is divided into two by an optical chopper, and one, the reference signal, is continuously checked by another photomultiplier. The relative intensity of the fluorescence signal and the reference signal is calculated with a microcomputer (J-3100GT, Toshiba Electronics, Tokyo, Japan).

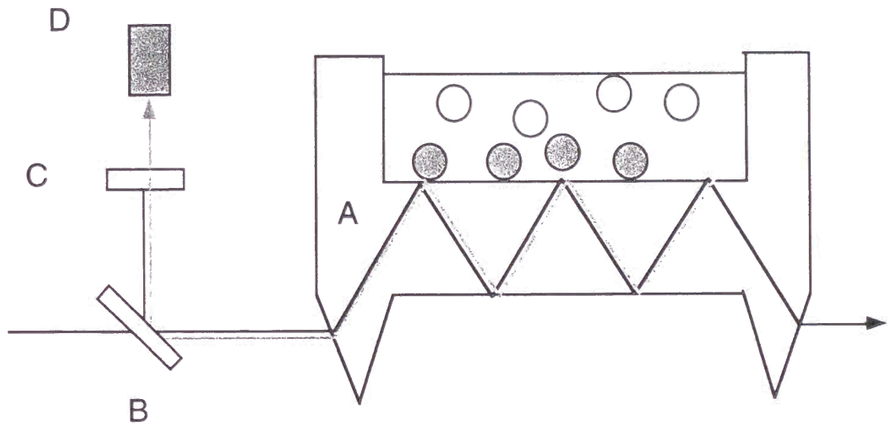

Figure 6-2 Schematic of the MIRF method.
Plain line, excitation beam; gray line, fluorescence; open circle, FITC-protein (without excitation); closed circle, FITC-protein (excited); A, optical wave guide with prisms; B, dichroic mirror; C, cut filter; D, detector.

6.2.2. Materials.

L-α-Distearoyl phosphatidylcholine (DSPC) was purchased from Sigma (St. Louis, MO). The hapten-doped lipids, N-2,4-dinitrophenyl-phosphatidylethanolamine, dipalmitoyl (DNP-DPPE) and N-dinitrophenyl-aminocaproyl-phosphatidylethanolamine, dipalmitoyl (DNP-cap-DPPE), were from Avanti Polar Lipids, Inc. (Aldbaster, USA). (Fig. 6-3) A monoclonal antibody, anti-DNP-IgE, was from Serotec (Oxford, England). Fluorescein isothiocyanate (FITC, Art 24 546, Aldrich, Milwaukee, WI) was used to label the antibody. Labeling was performed in a phosphate buffer (pH 9; 10 mM) overnight at 5°C. Free FITC was separated from the protein modified with fluorescein groups by GPC using a Sephadex G-25 column (2 i.d. x 30 cm) (mobile phase; pH7 phosphate buffer, 10 mM). The number of fluorescein groups per antibody molecule (F/P ratio) was determined by comparing the absorbance at 490 nm with the absorbance at 280 nm obtained from a UV spectrophotometer (U-3400; Hitachi, Tokyo, Japan). The F/P ratio of IgE used in this work was 3.5. Milli-Q water was used for the preparation of the sample solutions.

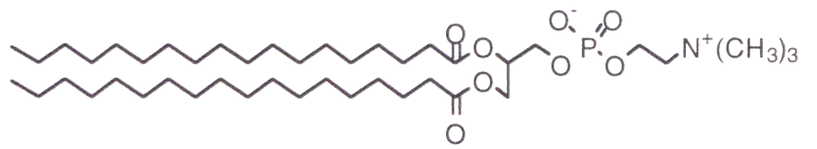

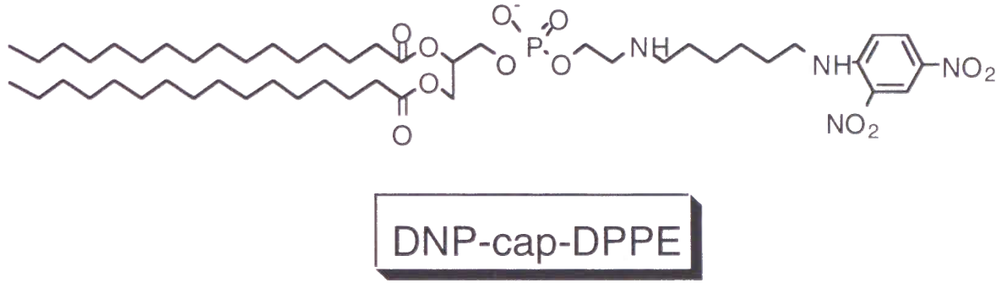

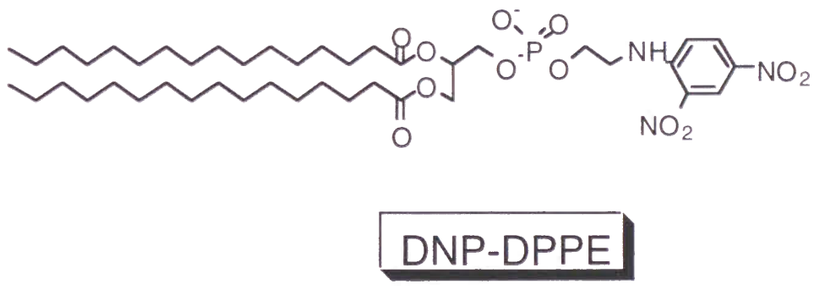

Figure 6-3 Structures of the lipids used in this work. L-α-distearoyl phosphatidylcholine (DSPC), N-2,4-dinitrophenylaminocaproyl-phosphatidylethanolamine, dipalmitoyl (DNP-cap-DPPE), N-2,4-dinitrophenyl-phosphatidyl-ethanolamine, dipalmitoyl (DNP-DPPE).

6.2.3. Preparation of Hapten-doped Lipid Monolayers.

The lipid solutions, having various lipid compositions (0-100 mol% of hapten-doped lipid; solvent, chloroform), were applied dropwise to the interface between air and deionized water in a Langmuir-Blodgett (LB) trough (Kyowa Kaimenkagaku Co., Ltd., Tokyo, Japan). To achieve equilibrium, the monolayer was left for 15 min., and was then slowly compressed until the surface pressure reached 35 mN/m. The monolayer was finally deposited on the waveguide mentioned above. The modified waveguides were stored in a desiccator for at least 1 day. From the surface pressure-area (π-A) curve, it was confirmed that the occupying coverage of the lipid was its critical value (42 Å^2 per molecule [17]) when the surface pressure was 35 mN/m.

6.2.4. Assay Procedure.

The antibody solutions were prepared with a phosphate buffer (pH7.0, 10 mM) and injected into the waveguide by means of an automatic pipetter (Microelectropette, Matrix Technologies, Lowell, MA) to keep the injection speed constant.

6.2.5. Calibration Experiment.

The calibration curve was produced in order to convert the signal intensity into the surface binding density of antibodies on the wave guide (C_s). (Fig. 6-4) The C_s value was obtained from the decrease in concentration of the solution above the cuvette, which could be evaluated from the fluorescence intensity at 520 nm (excitation, 480 nm) using a fluorescence spectrophotometer (F-410, Hitachi, Tokyo, Japan). The amount of antibodies bound to the monolayer (C_s) and the intensity of the fluorescence showed a linear relationship.

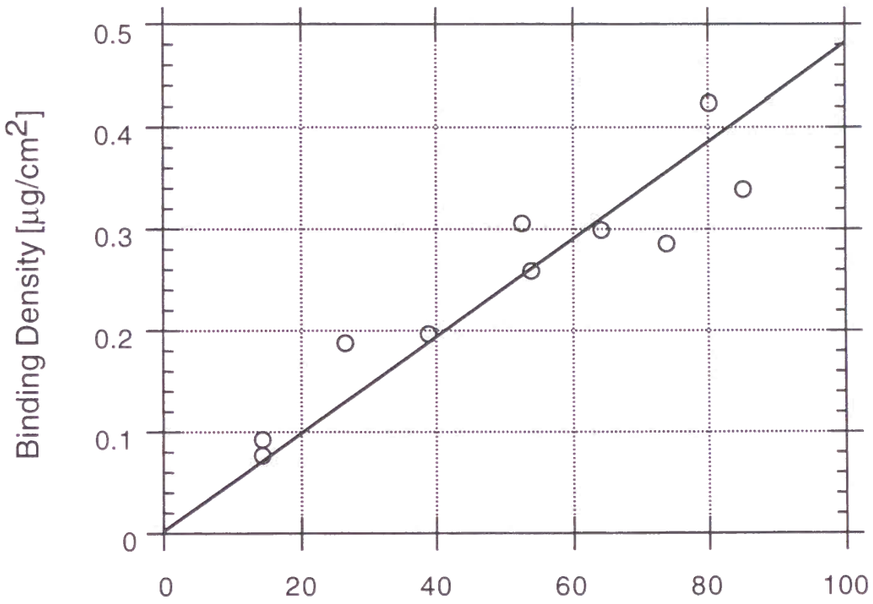

Figure 6-4 Calibration curve used for conversion of the signal intensity into the density of antibody bound to a hapten-doped lipid monolayer (DNP-cap-DPPE : DSPC = 10 : 90 [mol%]).

6.3. Results and Discussion

6.3.1. Effects of Hapten Density on the R Value and the Amount of Antibody Bound.

After injection of the antibody labeled with fluorescein groups (FITC-IgE) into the cell on which a hapten-doped lipid monolayer had been deposited beforehand, the fluorescence signal increased rapidly, as shown in Fig. 6-5 curves (b) and (c), whereas after injection into the cell that had been coated only with a DSPC monolayer, the fluorescence signal increased comparatively more slowly, as shown in Fig. 6-5 curve (a). The signal intensities almost leveled out within 50 sec. in all cases. A difference between signal curve (a), which was assigned to non-specific adsorption, and signal curves (b) and(c), which arose from the summation of the specific and non-s pecific binding, was observed clearly for various conditions.

The initial binding rate $(dC_s/dt)_0$, which was calculated from the initial slope of the fluorescence signal curve increased linearly with a concentration of proteins in the injected solution. The R value, which is the ratio of the experimental binding rate to the theoretical value for a diffusion-controlled binding, $(dC_s/dt)_{theor}$, given by eq. (6.1),[18] was evaluated by eq. (6.2).

$$dC_s/dt\ _{theor} = C_0(D/\pi t)^{0.5} \qquad (6.1)$$

$$(dC_s/dt)_0\ /\ (dC_s/dt)_{theor} = R \qquad (6.2)$$

where C_0 and D are the concentration and the diffusion coefficient of FITC-IgE (D = 3.7 x 10^{-7} cm^2s^{-1} at 20°C) [19], respectively. The R values obtained in this manner are shown in Fig. 6-6. At the low hapten density (0 ~ 10 mol%), the R value

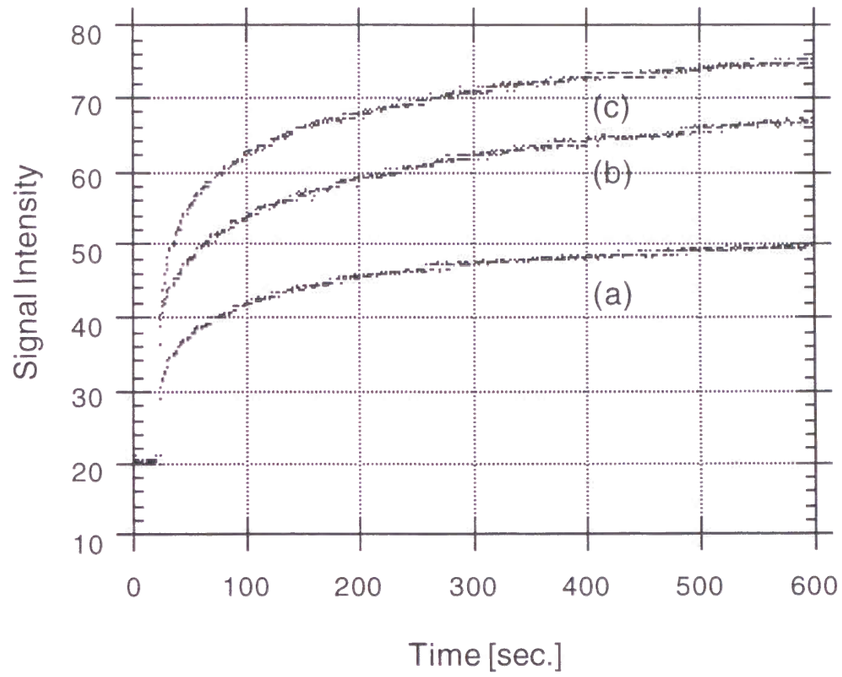

Figure 6-5 Comparison between the specific and non-specific binding curves ([antibody] = 50 mg/ml). Curve (a), fluorescence signal from non-specific binding of antibody to DSPC monolayer; curve (b), fluorescence signal from the sum of non-specific and specific binding of antibody to the hapten-doped monolayer (DNP-DPPE : DSPC = 10 : 90 [mol%]); curve (c), fluorescence signal from the sum of non-specific and specific and specific binding of antibody to the hapten-doped monolayer (DNP-cap-DPPE : DSPC = 10 : 90 [mol%]).

increased with hapten surface density. Above 20 mol%, the *R* value leveled out and there was no effect of hapten increase on the *R* value. It can be said that the rise in the *R* value with increase of hapten density reflects the presence of a specific immunological reactions between the antibody and the hapten.

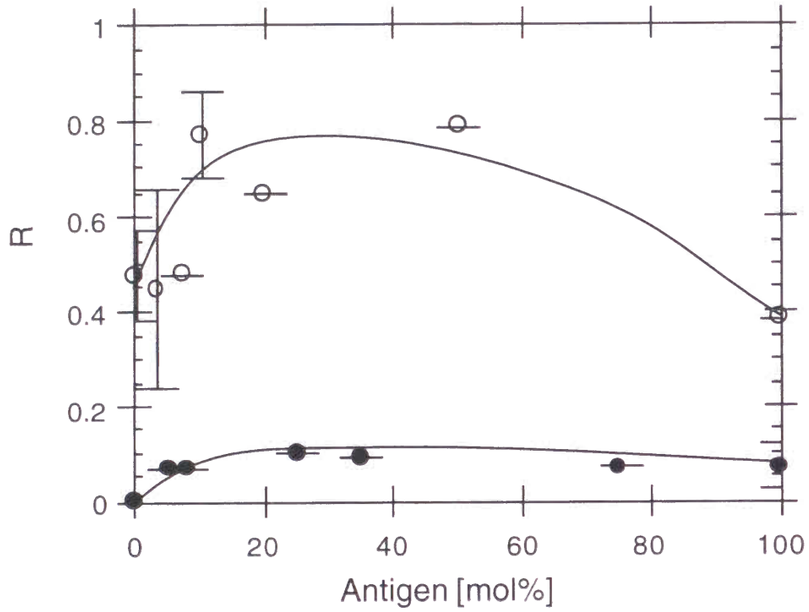

Figure 6-6 The R value for the specific binding of antibodies to antigens and haptens at various surface densities. Open circle; binding of anti-DNP-IgE to the DNP-doped lipid monolayer, filled circle; binding of anti-human serum albumin (HSA)-IgG to the PMMA surface modified with HSA and ovalbumin (from ref. 15).

We assume that two explanations may be given for the effect of the surface hapten density: antibody accessibility to the haptens and steric hindrance by the bound antibodies themselves.

As the surface hapten density increases, the space between the hapten-doped lipids decreases. When the density of haptens is low (0-10 mol%), the reduction of the space between the haptens raises the possibility of the meeting of an antibody and an hapten and accelerates the binding behavior of the antibody, whereas at higher doping densities (above 30 mol%), the space between the haptens is too small for the antibody to access and to bind tightly.

The second explanation, steric hindrance, is defined by the flexibility of the bound antibody. When the density of the haptens is low, judging from the size of the antibodies, the binding of the antibodies to the haptens is monovalent. The antibodies bound to the haptens, therefore, do not largely interfere with the access of another antibody to a hapten near them because of the flexibility of the monovalent bonds. When the density of the haptens is high, on the other hand, the binding of antibodies to the haptens can be bivalent. Pisarchick and Thompson [20] reported that at most antibody surface densities, 50-90 % of membrane-associated intact antibodies were attached to the surface at two antigen binding sites. The antibody that is bivalent is, therefore, fixed to two places on the interface, and the antibodies already bound obstruct the access of other antibodies to a hapten near them. The increase in the amount of antibodies that bivalently bind to the haptens, therefore, makes the binding of other antibodies difficult.

Next we measured the binding density of the anti-DNP-IgE to the hapten-doped lipid monolayer in the near-equilibrium state (600 sec. after the start of the binding experiment) (Fig. 6-7). True binding equilibrium could be attained several days later, and the trend shown in the figure was not greatly different from that in the true equilibrium state. Similar to the trend of the *R* values, the amount of bound antibody increased with the increase in the percentage of

hapten-doped lipid in the monolayer, and then leveled out. It was reported that if all the bound antibodies had a side-on binding position, the equilibrium binding density was 0.27 μg cm^{-2}.[19] The maximum binding density in this case was 0.24 μg cm^{-2} and about 80 % of the value described above.

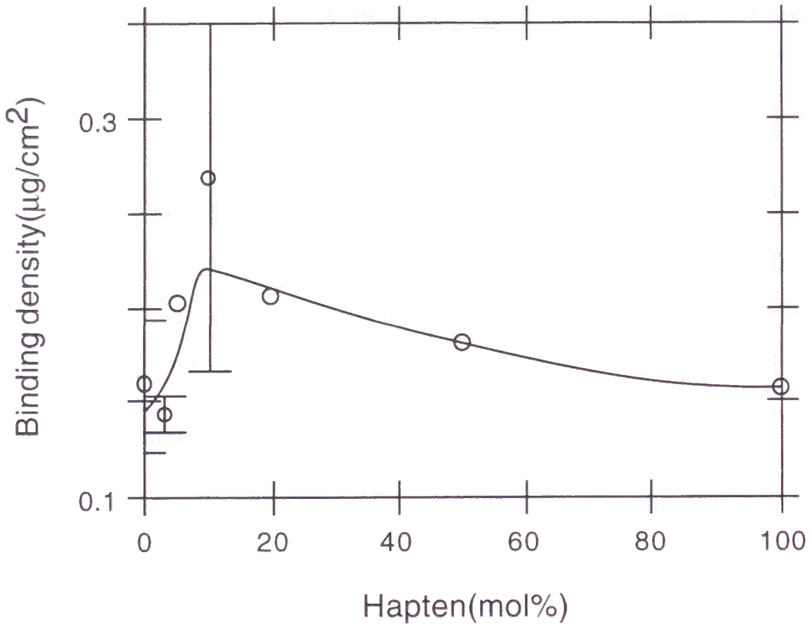

Figure 6-7 Binding density of anti-DNP-IgE to the lipid monolayer containing DNP-cap-DPPE.

6.3.2. Effectsof the Length of Spacer on Binding Process.

The dependence of the binding rate on the length of the spacer was estimated by comparing the binding behavior of antibodies to lipid monolayers which had different spacer lengths between the amino group of the lipid and the hapten (dinitrophenyl group). One had a spacer of six carbon chains (DNP-cap-DPPE), the other had no spacer (DNP-DPPE). Different binding behaviors were observed as shown in Fig. 6-5, curves (b) and (c) (binding curve) and Fig. 6-8 (R vs.

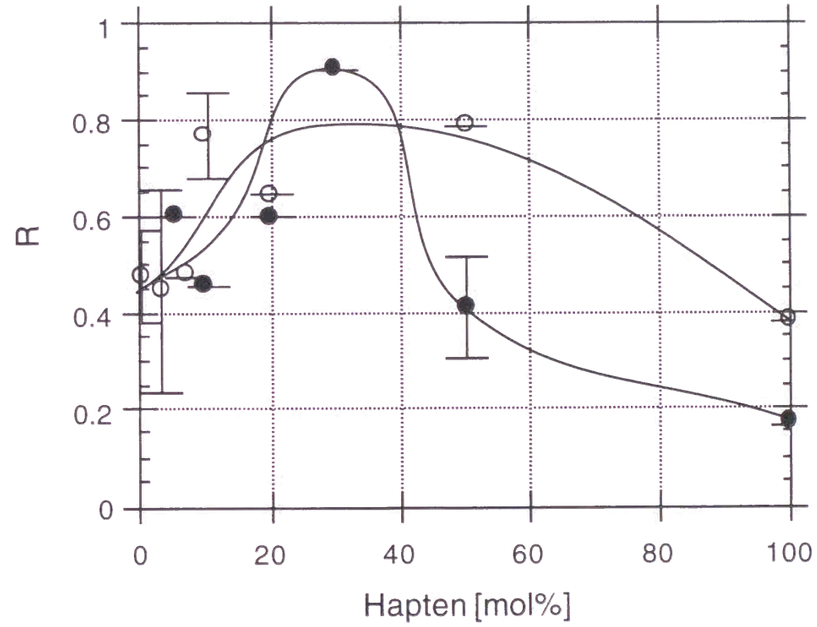

Figure 6-8 The R value for the specific binding of anti-DNP-IgE to the DNP-doped lipid monolayer.
Open circle; binding of antibody to the DNP-doped lipid monolayer with a six-carbon spacer, filled circle; binding of antibody to the DNP-doped lipid monolayer without spacer.

DNP density). The most probable reason for this is that the dinitrophenyl group (DNP group) of the lipid with the spacer partly extends beyond the surface of the lipid monolayer, whereas the DNP group of the lipid without the spacer was at the surface. Therefore DNP-cap-DPPE (with spacer) is more accessible to the antibody than DNP-DPPE (without spacer).

6.3.3. Comparison with Chapter 5.

In Chapter 5, we examined the specific binding processes of antibodies to a flat surface of PMMA modified with an antigen protein (human serum albumin (HSA)).[15] When the surface was covered with HSA, the anti-HSA-antibody bound quickly, whereas there was no significant binding of the antibody to the surface modified with ovalbumin (OVA). The *R* value for the surface of the cuvette having various HSA : OVA ratios was shown for comparison in Fig. 6-6. When the percentage of occupation by HSA on the surface was zero, there was no binding, whereas in the presence of 25 mol% HSA, the *R* value reached a maximum (0.10), and then gradually decreased. The *R* values for the HSA and anti-HSA-antibody system were lower than those for the system of hapten-doped lipid monolayers and anti-DNP-IgE. This phenomenon suggests that the haptens in the monolayer system were advantageously oriented upward, and the immunogens in the HSA system were disordered in contrast.

In addition, we measured the near-equilibrium binding density 600 s after the start of the binding experiment at various percentage of occupations by the haptens (Fig. 6-7). Similar to the HSA and anti-HSA-antibody system previously examined,[15] the C_s value increased with the increase in the percentage of antigens (in this study, haptens; the DNP group) on the cuvette surface, and the C_s values for two systems were of the same order. The spatial orientation of antigens (haptens) does not seem to affect the near-equilibrium binding density of the antibodies so much, if the surface concentration of antigens (haptens) is

sufficiently high. The most effective factor for deciding the equilibrium binding density in this case may be the size of antibodies.

6.4. Conclusion

Both the binding rate and the binding density of antibodies to haptens at the lipid-solution interfaces were affected by surface conditions such as density and orientation of the haptens. At a low surface concentration (0-20 mol%) of haptens, the initial binding rate of the antibody to the hapten-doped lipid monolayer increased rapidly, and leveled off at a higher surface density, which indicates that the binding of the antibodies is affected by the space required for the antibodies to access the haptens. The environments of the antigens, such as the spatial structure and orientation, do not significantly affect the surface concentration of the bound antibodies.

References

(1) Voet, D.; Voet, J.G., Biochemistry, John Wiley, New York, (1990).

(2) Pecht, I.; Lancet, D. *Mole. Biol. Biochem., Biophys* ,. **1977**, 306.

(3) Kulczycki, Jr. A.; Metzger, H. *J. Exp. Med.* **1974**, *140*, 1676.

(4) Kobayashi, M.; Nakanishi, M.; Tsuboi, M. *J. Biochem.* **1982**, *91*, 407.

(5) Tashiro, Y.; Kataoka, K.; Sakurai, Y. *J.Colloid Interface Sci.* **1990**, *66*, 140.

(6) Kitano, H.; Nakamura, K.; Hirai, Y.; Kaku, T.; Ise, N. *Biotechnol. Bioeng.* **1988**, *31*, 547.

(7) Nakamura, K.; Hirai, Y.; Kitano, H.; Ise, N. *Biotechnol. Bioeng.* **1987**, *30*, 216.

(8) Hasegawa, M.; Kitano, H. *Biotechnol. Bioeng.* **1991**, *37*, 608.

(9) Hirschfeld, T. *Can. Spectrosc.* **1965**, *10*, 128.

(10) Tilton, R. D.; Robertson, C. R.; Gast, A. P. *Langmuir* **1991**, *7*, 2710.

(11) Golander, C. -G.; Hlady, V.; Coldwell, K.; Andrade, J. D. *Colloids and Surfaces* **1990**, *50*, 113.

(12) Beissinger, R. L.; Leonard, E. F. *ASAIO J.* **1980**, *3*, 160.

(13) Sutherland, R. M.; Dähne, C.; Plase, J. F.; Ringrose, A. S. *Clin. Chem.* **1984**, *30*, 1533.

(14) Hasegawa, M.; Kitano, H. *Langmuir* **1992**, *8*, 1582.

(15) Tanimoto, S.; Kitano, H. *Langmuir* **1993**, *9*, 1315.

(16) Kitano, H.; Ohno, K. *Langmuir* , **1994**, *10*, 4131.

(17) R. R. C. New in "Liposomes: A Practical Approach" (R. R. C. New, Ed.) IRL Press (1990) p.9

(18) MacRitchie, F. *Adv. Protein Chem.* **1978**, *32*, 283.

(19) Baskin, A.; Lyman, D. J. *J. Biomed. Mater. Res.* **1990**, *14*, 393.

(20) Pisarchick, M. L.; Thompson, N. L. *Biophys. J.* **1990**, *58*, 1235.

Appendix
List of Publications
Acknowledgements

Appendix

The program for evanescent wave light scattering microscope (EVLSM) technique used in Part I of this thesis was edited by following to the format of N88-BASIC for NEC computer, and shown below.

```
5     'SAVE "A:tan4",A:'*****EVLSM PROGRAM*edited by TAN****
100 DEFINT D
110  OPTION BASE 1
120 DIM D(32766)
130 SCREEN 3:CONSOLE 0,25,0,1,1:WIDTH 80
140 PRINT :INPUT " [0] T.D : [1] T.I ";A
150 PRINT"[0] 0.1  [1] 0.2  [2] 0.4  [3]0.8
160 PRINT"[4] 1    [5] 2    [6] 4    [7]8
170 PRINT"[8] 10   [9] 20   [10]40   [11]80
180 PRINT"[12]100  [13]200  [14]400  [15]800
190 PRINT"[16]1000 [17]2000 [18]4000 [19]8000
200 PRINT :INPUT " CLOCK RATE ( 0 -------- 19 )";B
210 PRINT :INPUT " RAM DATA [0]1K[1]2K[2]4K[3]8K[4]16K[5]32K[6]64K" ;C
220     OUT 218,0:OUT 219,0:OUT 220,0
230     OUT 219,C+B*8
240     OUT 218,A*32:OUT 218,A*32+4:OUT 218,A*32
250     OUT 218,A*32+64
260     OUT 218,A*32
270 'pRINT "  WAIT ";
280 IF (INP(217) AND 128)=0 THEN 270
290 N=0
300     OUT 218,128:OUT 218,128+64
310     OUT 218,128
320     OUT 218,2:OUT 218,0
330 N=N+1
340     OUT 218,1
```

```
350 D(N)=INP(217)*256+INP(216)
360 IF (INP(217) AND 128)=0 THEN 390
370 IF (INP(217) AND 128)=128 THEN 480
380 IF D(N)>=32767 THEN PRINT "COUNT OVER
390 PRINT D(N),;
400 N=N+1
410     OUT 218,0:OUT 218,2
420 IF (INP(217) AND 128)=128 THEN 480
430 D(N)=INP(217)*256+INP(216)
440 IF D(N)>=32767 THEN PRINT "COUNT OVER
450 PRINT D(N),;
460 N=N+1:OUT 218,0
470 IF (INP(217) AND 128)=0 THEN 340
480 PRINT "DATA NUMBER=";N
490 INPUT "file name?";F$
500 OPEN F$ FOR OUTPUT AS #1
510 FOR I=1 TO N
520 PRINT #1,D(I)
530 NEXT
540 CLOSE :PRINT "storage is finished!"
550     OUT 219,0:OUT 218,0
560 END
```


List of Publications

I. Parts of the present thesis have been or are to be published in the following journals.

Chapter 2
Tanimoto, S.; Matsuoka, H.; Yamaoka, H. *Colloid Polym. Sci.* **1995**, *273*, 1201.

Chapter 3
Tanimoto, S.; Takahashi, K.; Matsuoka, H.; Yamaoka, H. *Colloids and Surfaces*, to be submitted.

Chapter 4
Tanimoto, S.; Matsuoka, H.; Yamauchi, H.; Yamaoka, H. in preparation.

Chapter 5
Tanimoto, S.; Kitano, H. *Langmuir* **1993**, *9*, 1315.

Chapter 6
Tanimoto, S.; Kitano, H. *Colloids and Surfaces B* **1995**, *4*, 259.

II. Other publications not included in this thesis.

(about evanescent wave dynamic light scattering (EVDLS) study)
Matsuoka, H.; Morikawa, H.; Tanimoto, S.; Kubota, A.; Naito, Y.; Yamaoka, H. *Colloid Polym. Sci.* to be submitted.

Acknowledgements

The present thesis is based on the studies carried out by the author at the Department of Polymer Chemistry, Faculty of Engineering, Kyoto University, Kyoto 606, Japan from 1991 to 1997 under the direction of Professor Hitoshi Yamaoka.

The author would like to express his sincere gratitude to Professor Hitoshi Yamaoka, Department of Polymer Chemistry, Kyoto University, for his guidance, advice and encouragement throughout the course of this work.

The continuous guidance, valuable discussion, advice and comments of Assistant Professor Hideki Matsuoka, Department of Polymer Chemistry, Kyoto University are gratefully acknowledged.

The author is indebted to Professor Hiromi Kitano, Department of Chemical and Biochemical Engineering, Toyama University, for his valuable advice, suggestion and discussion.

The author wishes to thank Dr. Kozo Matsumoto, Department of Polymer Chemistry, Kyoto University, for his valuable suggestion and comments.

Thanks are given to Messrs. Hirofumi Morikawa, Yoshiharu Naito, Akira Kubota, Katsunori Takahashi, and Hiroshi Yamauchi for their assistance in the experimental work.

The author also thanks his colleagues in Yamaoka Laboratory for their encouragements and continuous friendship.

November 1997

Satoshi Tanimoto